Scientific Research Publishing

Advances in Bioscience and Biotechnology, 2026, 17(8), 376-417
https://www.scirp.org/journal/abb
ISSN Online: 2156-8502
ISSN Print: 2156-8456

Homeostasis at the Edge of Order: Cancer, Modulated Electro-Hyperthermia, and the Role of 1/f Noise

Andras Szasz[1,2]

[1]Biotechnics Department, Hungarian University of Agriculture and Life Sciences, Budaors, Hungary
[2]XAX Consulting LLC, Lincoln, MA, USA
Email: prof.szasz@gmail.com

How to cite this paper: Szasz, A. (2026) Homeostasis at the Edge of Order: Cancer, Modulated Electro-Hyperthermia, and the Role of 1/f Noise. *Advances in Bioscience and Biotechnology*, **17**, 376-417.
https://doi.org/10.4236/abb.2026.178024

Received: July 2, 2026
Accepted: August 28, 2026
Published: August 31, 2026

Abstract

Homeostatic regulation ensures a dynamic equilibrium, maintaining the constancy of an organism's internal environment despite continuous external fluctuations and internal metabolic demands. Homeostasis reflects a balance between stability and adaptability. This review explores how the biophysics operating near a second-order phase transition may be an evolved property of living systems, enabling maximal sensitivity, dynamic range, and information processing. Growing evidence suggests that biological systems operate near critical points, on the "edge of chaos". Departure from criticality manifests in pathological states such as cancer, where the breakdown of cooperative cellular order may be interpreted as a transition away from the critical regime. The modulated electro-hyperthermia (mEHT) is a therapeutic intervention whose biophysical action can be understood through the lens of membrane-level dynamics in tumor cells. The homeostatic dynamics exhibit 1/f noise, a hallmark signature of self-organized criticality (SOC) in homeostasis, and it is a practical diagnostic indicator of physiological health versus disease. Together, these threads weave a coherent biophysical narrative: growing theoretical and experimental evidence suggests that many biological systems operate near criticality, and understanding this edge has profound implications for both fundamental biology and clinical medicine. One of the most powerful conceptual frameworks in modern biophysics is statistical mechanics, whose dynamics can be characterized by the Ising model, a useful tool for describing phase transitions at the boundary between order and chaos. Its capacity to capture collective behavior, long-range correlations, and phase transitions near a critical point renders it uniquely suited to modeling phenomena as diverse as neural dynamics, gene expression networks, cellular communication, and tissue organization, making it a suitable

modeling tool for studying cancer development and prevention. My objective is to show the behavior of a living system at a phase transition and the corrections that arise when the system deviates from this delicate state, and connect these ideas to cancer and therapeutic intervention.

Keywords

Ising Model, Spin Glass, SOC, mEHT, Pink Noise, Edge of Chaos, Nonthermal Processes, Homeostasis, Stochastic Resonance

1. Introduction—Phase Transitions and Criticality in Biological Matter

Physics and biology have long maintained a productive, if sometimes uneasy, relationship. The application of thermodynamic concepts to living systems gained momentum throughout the twentieth century, yet it was the recognition that biology is not merely thermodynamics in equilibrium, but a complex, nonequilibrium, self-organizing phenomenon, that catalyzed a new era of biophysical inquiry. At the heart of this inquiry lies a deceptively simple question: are the coordinated behaviors of cells, tissues, and organisms best understood as emergent properties arising near a phase transition?

We can address the challenges by examining the robust behavior that results from this complexity: self-organization and its subsequent self-similarity [1]. The complexities of living structures exhibit universal behavior: they are self-organized [2]. In recent decades, various approaches have been developed to describe the complexity of systems in terms of self-organization [3]-[5]. This peculiar structure is built according to relatively simple self-similarity rules [6]. The dynamism of the structure is determined by the system's symmetries [7] and constructs a self-managed spatiotemporal fractal network [8] leading to a typical bioscaling behavior in living material [9]. Consequently, the similarity of living species enables allometric scaling across 24 orders of magnitude from the smallest to the largest biological objects [10].

Living systems are open, dynamical structures that engage in random, stationary, and stochastic self-organizing activities [11]. The self-organizing technique generates a spatiotemporal fractal structure that is self-similar in both space and time [12]. The emerging fields of bio-scaling [13] and network analysis [14] extend detailed analyses. The characteristic stochastic (probabilistic) behavior of living matter is related to the intrinsic bifurcation in the entirety of the living organization. The basic bifurcation mechanism can be represented by a non-linear double-well potential for chemical reactions [15] [16], leading to a chaotic arrangement.

Cells can undergo a phase transition, altering their structure and chemical bonds [17] [18], without a change in temperature. The quantum mechanics and resonances within chemical bonds are primarily non-equilibrium thermody-

namic states, highlighting the combined influence of thermal and nonthermal energy components [19]. The external electric field nonthermally promotes cellular fission at low [20] and high [21] frequencies, and its application holds promise in cancer therapy [22].

The complexity of living systems is at a crucial point. Since biological systems experience vital fluctuations near their equilibrium states, life functions at the "edge of chaos" [23] [24], owing to its complex stochastic interactions [25]. The phrase, originating from dynamical systems theory, describes a specific regime that is not the fixed regularity of crystalline order nor the chaotic formlessness of pure randomness, but rather the narrow transition zone between these two states.

The term "edge" fits well. A literal edge exists as a one-dimensional boundary within a two-dimensional landscape; it has no width but only a direction. Similarly, edge-of-chaos dynamics are limited: this regime is a narrow manifold within a vast array of potential states, requiring the system to continually expend energy to stay on it. This explains why living systems are energetically costly. Maintaining this critical state isn't free; it demands a constant influx of energy and information, much like any far-from-equilibrium dissipative structure. The edge of chaos isn't simply a middle ground between order and disorder or a diluted form of either. Instead, it constitutes a distinct third regime, with emergent properties that cannot be derived from the characteristics of the neighboring regimes. Criticality differs fundamentally from subcriticality and supercriticality, with systems at this edge showing long-range correlations, scale-invariant fluctuations, and heightened sensitivity to inputs that would be ineffective in either adjacent regime.

Operating at the boundary between order and chaos optimizes biological function because it enables signals, whether electromagnetic, biochemical, mechanical, or electrochemical—to propagate through the system in ways that neither highly ordered nor purely chaotic regimes allow. In a highly ordered medium with strong damping, a signal starting at one point decays before reaching another, as the system's rigidity absorbs the perturbation locally. Conversely, in a purely chaotic regime, a signal is quickly overwhelmed by the system's own noise, making it indistinguishable from background activity. Only at the critical boundary does a signal effectively travel and persist, transmitting information across the system with enough fidelity, while remaining within a stochastic environment that permits modulation, gating, and selective responses.

This fundamental dynamical principle underpins all activities of the organism. Whether it's a propagating action potential, a hormonal cascade, a calcium wave through tissue, or electromagnetic coupling between cells, none would function in a rigid or entirely chaotic medium. Instead, they rely on the medium being critical. This same principle explains the organism's remarkable sensitivity to weak stimuli: at the brink of chaos, minor disturbances can trigger significant, organized responses because long-range correlations enable local events to acti-

vate widespread structures. This capacity allows organisms to detect and respond to faint signals—like pheromones near threshold levels, photons at the limit of single-quanta detection, or vibrations close to the cochlea's noise floor—that a less critical system couldn't perceive. Life exists at this edge; it's the only place it can thrive.

The Ising model is among the most precise statistical mechanical models for understanding phase transitions. While it can represent the criticality of life, it doesn't fully encompass reality; instead, it depicts how life behaves at its "edge of chaos."

2. The Ising Model: Mathematical Foundations and Biological Mapping

2.1. The Model and Its Biological Equivalence

The Ising model, introduced by Wilhelm Lenz and solved in one dimension by Ernst Ising in 1925 [26], and later extended to two dimensions by Lars Onsager in 1944 [27], and recently shows an intuitive [28] and an algebraic approximation in three dimensions by the author in 2026 [29], describes a lattice of binary variables ($s_i = \pm 1$, in magnetism, these are spins) interacting via nearest-neighbor coupling. Despite its simplicity, the model exhibits a rich phase transition between an ordered and disordered state, separated by a critical temperature T_c at which the magnetic system displays scale-free fluctuations, long-range correlations, and maximal susceptibility.

The notion that biological systems may operate near criticality was first suggested in the context of neural networks [30] and later given strong empirical grounding [31]. It has been demonstrated that cortical networks exhibit neuronal avalanches with power-law statistics consistent with a critical branching process. Subsequently, [32] applied maximum-entropy methods rooted in the Ising framework to retinal ganglion cell populations, finding that the biological data sit strikingly close to the critical point of a pairwise interaction model. These findings have since been generalized to gene regulatory networks, immune repertoires, flocking birds, and even the human microbiome, suggesting that criticality may be a universal organizing principle of complex living systems.

In the classical magnetic picture, the canonical Ising Hamiltonian ($\mathcal{H}$) describes a system of N spins on a lattice, with pairwise interactions and an external field:

$$\mathcal{H} = -J \sum_{\langle i,j \rangle} s_i s_j - h \sum_i s_i \tag{1}$$

where J is the exchange coupling ($J > 0$ for ferromagnetic alignment), h is an external magnetic field, and the first sum runs over nearest-neighbor pairs $\langle i, j \rangle$. The partition function

$$Z = \sum_{\{s\}} \exp\left(-\frac{\mathcal{H}}{k_B T} \right) \tag{2}$$

encodes all thermodynamic information, where $k_B \cong 1.39\times10^{-23}\,\frac{\mathrm{J}}{\mathrm{K}}$ is the Boltzmann constant, and T is the temperature on the absolute (Kelvin) scale. It can be shown that in the thermodynamic limit at $T = T_c$, the free-energy density becomes non-analytic at Tc, where the correlation length and susceptibility diverge.

This simple model became the fundamental model of statistical physics, showing the importance of nondeterministic statistical phenomena.

The Ising framework can be interpreted biological terms. Cells within tissue communicate through biochemical and electrical signals. These interactions create collective regulatory states, analogous to spin alignment. The physical variables and their biological analogs are shown in Table 1.

Table 1. The physical variables and their biological analogs.

Physical variable	Biological analogue
spin state (s_i)	cellular functional state
interaction (J)	cell-cell communication
temperature (T)	metabolic noise
field (h)	environmental stress
magnetization (M)	tissue functional order

While in the Ising model, temperature (T) controls disorder vs. order, this magnetic model may simulate numerous statistical parameters of the biological systems, connected to its dynamic stability, the homeostasis. Thermodynamic parameters, such as temperature, susceptibility, order parameter, correlation length, and specific heat, serve as effective control parameters that quantify noise, variability, or regulatory balance in a biological system. The critical exponents then describe how observables (correlations, fluctuations, responses) scale as the system approaches its homeostatic critical point, where the control balances at the "edge of chaos". In biology. The mapping to the Ising model is not literal but provides a coarse-grained, phenomenological framework that captures collective behavior and phase transitions. The analogous quantity of temperature is an effective parameter (T_{eff}), which can represent stochastic fluctuations (gene expression noise, ion-channel noise), metabolic activity/ATP-driven fluctuations, environmental variability, and regulatory noise in signaling networks (Figure 1). Considering the cellular-automaton-like spatiotemporal patterns differences between frozen order, edge of chaos (fractal scale-free clusters), and turbulent chaos (random noise), the complexity-vs-control-parameter curve is a narrow peak where life operates. The sensibility (susceptibility) χ as a Lorentzian-style peak diverges at T_{eff} and is essentially zero a little farther on either side. Together, these are the canonical thermodynamic signatures of a critical point: the order parameter changes continuously across T_{eff} (no jump = second-

order), while the susceptibility, the response to an infinitesimal external field, diverges. Note that this version of the order-parameter curve is symmetric (going negative above T_{eff}), which is a mean-field-like portrait suitable for an Ising magnet in a vanishingly weak field that selects sign. A useful interpretation is:

$$T_{eff} \sim \frac{\text{noise amplitude}}{\text{interaction strength}} \begin{cases} T_{eff} < T_{tr} & \text{overly ordered}\left(\text{rigid, frozen dynamics}\right) \\ T_{eff} > T_{tr} & \text{overly disordered}\left(\text{uncorrelated, noisy}\right) \\ T_{eff} \approx T_{tr} & \text{optimal balance} \Rightarrow \text{homeostasis} \end{cases} \quad (3)$$

The critical point (T_{tr}) separates ordered and disordered phases, which biologically is the point where the system has maximal adaptability, maximal susceptibility, and long-range coordination. It can be interpreted in various homeostatic controls, among those the

1) neural systems → edge of synchronization;

2) cardiac dynamics → healthy variability;

3) cell populations → coordinated but flexible behavior;

4) membranes → lipid criticality (raft formation).

These are precisely the properties of criticality and their biological analogs that have attracted intense interest in the biophysics community.

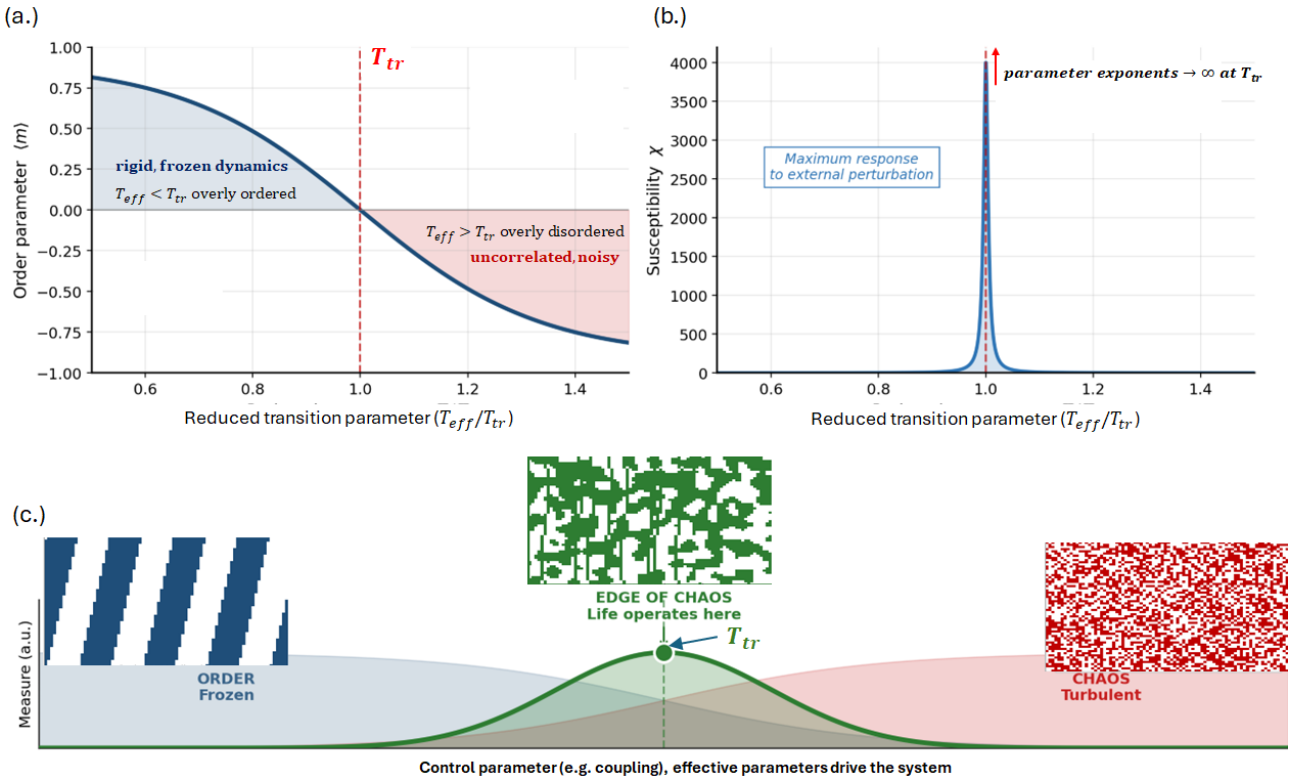

Figure 1. Two signatures of a second-order phase transition. (a) The order parameter has a smooth crossover. (b) The physical exponents (as corresponding biophysical) diverge at the critical point, at healthy homeostasis. (c) A living system operates at the narrow boundary between frozen (ordered) and turbulent (chaotic) states.

The optimal regime of a living object lies near the critical point, where the sys-

tem maintains high responsiveness, long-range coordination, and flexible adaptation.

Near the critical transition temperature (T_{tr}), the correlation length ξ diverges as $\xi \propto \left|T_{eff} - T_{tr}\right|^{-\upsilon}$ (with $\upsilon = 1$ in two dimensions (2D)), and the mean-field magnetization vanishes as $\langle m \rangle \propto \left|T_{eff} - T_{tr}\right|^{\beta}$ ($\beta = 1/8$ 2D), and susceptibility diverges as $\chi \propto \left|T_{eff} - T_{tr}\right|^{-\gamma}$ [33].

When translating these variables into a tissue-level or homeostatic context, the biological equivalence of the above parameter model, the thermodynamic concepts map to systemic biological regulation:

- Temperature, as an effective actor (T_{eff}) equal to the systemic stochasticity and noise in biology. Here the T does not merely represent thermal heat; it represents the aggregate stochastic noise of the system, fluctuations in metabolic availability, genetic expression, or environmental stressors. Lower T_{eff} favors rigid order (pathological synchronization), while higher T_{eff} drives random disorder (system failure). Healthy homeostasis is poised precisely at T_{tr}, maintaining an optimal balance of order and adaptability.
- Magnetization ($\langle m \rangle = \langle s_j \rangle$) represents the homeostatic order parameter. Biologically, $\langle m \rangle$ is the macroscopic order parameter that defines the collective state of the tissue. A high $|m|$ indicates high synchrony or coherent behavior (e.g., a highly ordered, rigid tumor microenvironment). A transition at T_{tr} signifies a shift in tissue phase, such as the breakdown of pathological coherence.
- Magnetic field (h) is the global modulating intervention. It represents an exogenous driving force or systemic intervention that breaks symmetry. In an oncological context, $\mathbf{h}$ is directly analogous to localized, specific physical interventions, like modulated electro-hyperthermia (mEHT) or targeted pharmacological therapies. It exerts a systemic bias, forcing the discrete units (s_j) to align with a new energetic minimum, thereby disrupting local pathological equilibria.
- Coupling (J) is the notion of intercellular connectivity. This is the biological communication network (e.g., gap junctions, cytokine signaling, local electrical coupling). In a malignant state, J is often fundamentally altered, isolating the tumor from the systemic homeostatic network.

The critical exponents around T_{tr} also have biological equivalence. Near the critical point T_{tr}, the behavior of the system is dominated by long-range correlations rather than local interactions. The thermodynamic variables scale according to power laws dictated by critical exponents. Let the reduced temperature be $t = \frac{T_{eff} - T_{tr}}{T_{tr}}$, to characterize the relative deviation from T_{tr}. With this notation, the biological equivalence of the critical exponents is as follows:

- The order parameter is the exponent β ($m \propto t^{-\beta}$ for $T_{eff} < T_{tr}$) defines how rapidly the tissue's coherent state (e.g., the rigid equilibrium of a tumor mass) collapses as the system is pushed toward criticality, but $\langle m \rangle \to 0$ at criticality, not diverge.

- The susceptibility exponent $\propto \left|T_{eff} - T_{tr}\right|^{-\gamma}$ where ($\chi = \frac{\partial m}{\partial h}$) is the tissue's responsiveness to the external intervention (**h**). As the system approaches T_{tr}, susceptibility diverges. This is highly relevant therapeutically: at the critical point, the biological network becomes exquisitely sensitive to extremely low-energy perturbations (such as specific modulated frequencies), meaning minimal external force is required to induce a massive shift in the collective state.
- The correlation length exponent $\xi \propto \left|T_{eff} - T_{tr}\right|^{-\upsilon}$ is the correlation length (ξ) defines the physical distance over which one cell's state influences another's. At T_{tr}, $\xi \to \infty$, meaning local fluctuations propagate globally. This scale-free correlation is the origin of the $1/f$ noise (where f is the frequency) observed in healthy homeostasis; the system acts as a unified whole rather than isolated parts.
- The specific heat exponent $C \propto \left|T_{eff} - T_{tr}\right|^{-\alpha}$ shows how the specific heat maps to the variance in energy fluctuations (or metabolic demand). A divergence at T_{tr} indicates massive fluctuations in resource utilization as the biological network attempts to reconfigure its state, a hallmark of a system undergoing a forced phase transition out of a locked equilibrium.
- The dynamical critical exponent $\tau \propto \xi^{z} \propto \left|t\right|^{-z\upsilon}$ describes the critical slowing down of the processes. As a biological system nears a tipping point (like the collapse of a tumor's local homeostasis), its recovery time from small perturbations (τ) diverges. The network loses its resilience and responds sluggishly to stress, making it highly vulnerable to continuous, modulated external interventions just before the phase transition.

2.2. Nonthermal Processes

The nonthermal effects are thermodynamically possible, as shown by the Gibbs free energy (G), which is usually counted in chemical reactions in biomaterials. To study the nonthermal pathways. G determines the spontaneity of processes under constant temperature and pressure. The differential form for a dielectric system is:

$$\Delta G = -S\Delta T + V\Delta p + \sum_i \mu_i \Delta N_i - \boldsymbol{P}\Delta\boldsymbol{E} - \boldsymbol{M}\Delta\boldsymbol{H} \tag{4}$$

If we assume a hypothetical scenario where the bulk temperature and macroscopic pressure are held completely constant (strongly thermostated, so $\Delta T = 0$ and $\Delta p = 0$), the equation simplifies to:

$$\Delta G = \sum_i \mu_i \Delta N_i - \boldsymbol{P}\Delta\boldsymbol{E} - \boldsymbol{M}\Delta\boldsymbol{H} \tag{5}$$

This mathematically shows that formally, filed terms enter the free-energy differential alongside the thermal term, so an applied field can in principle shift free energy at fixed bulk temperature, even if there is absolutely zero change in temperature, applying a changing electric ($\Delta\boldsymbol{E}$) of magnetic ($\Delta\boldsymbol{H}$) field will change the free energy of the system, which in turn must drive changes in polarization ($\boldsymbol{P}$), magnetization ($\boldsymbol{M}$) and chemical composition ($\mu_i \Delta N_i$) as the system

seeks a new minimum energy state. Electromagnetic energy is consumed by forcing chemical reactions, altering molecular configurations, and altering electrochemical gradients through pathways not reducible to bulk heating. The nonthermal processes do not exclude thermal effects; they involve interactions that the heat cannot achieve [34]. The nonthermal molecular excitations point to the biomatter's natural heterogeneities [35].

To model chemical reactions or varying molecular concentrations (e.g., oxygenation or glucose gradients in a microenvironment), we can map the Ising model onto a "lattice gas" model, which, similarly to the above, admits a 3D approximation [28]. Here instead of $s_j = \pm 1$ states, we define a discrete state variable based on chemical occupation or conformational state, $n_j \in \{0,1\}$. Introducing the chemical potential (μ_c), which represents the energy required to add or remove a specific molecule or alter a localized chemical state, the transformed chemical Hamiltonian becomes:

$$\mathcal{H}_{chem} = -J\sum_{\langle i,j\rangle} n_i n_j - \mu_c \sum_i n_i \tag{6}$$

Its biological meaning of the coupling J represents cooperative chemical binding or allosteric interactions between neighboring cellular receptors. If μ_c is highly positive (e.g., an abundance of resources or a highly acidic extracellular pH driving a specific cellular response), the system is strongly biased toward the $n_i = 1$ state, regardless of the thermal noise (T). Note that the T Noise is not only thermal heat; it is a stochastic noise of the system, fluctuations in metabolic availability, genetic expression, or environmental stressors, so it is not only the temperature, as the standard meaning in classical thermodynamics.

Standard thermodynamics treats an external magnetic or electric field as an additional contribution to the bulk energy that ultimately thermalizes (heating the system). However, nonthermal interventions, such as highly specific modulated radiofrequencies, do not primarily raise the bulk temperature T. Instead, they act as a time-dependent, targeted field that interacts selectively with the dipole moments or membrane-potential states of the cells, thereby introducing nonthermal aspects. Introducing a non-thermal driving field, $E_{nT}(t)$, which couples specifically to the susceptibility (γ_i) of the discrete unit i.

$$\mathcal{H}_{nT} = -\sum_i \gamma_i E_{nT}(t) n_i \tag{7}$$

This represents an externally applied, symmetry-breaking force that bypasses systemic thermal regulation. Because malignant or stressed tissues often possess different membrane physical properties (altered dielectric constants or lipid raft densities), γ_i varies between healthy and pathological cells. The non-thermal field selectively forces the pathological cells out of their local equilibrium, driving them toward a phase transition (apoptosis) without requiring a massive increase in systemic T.

Taking the chemical changes also into account in a real biological network, the communication between cells (the coupling J) is not a fixed structural con-

stant. It is dynamically gated by the chemical environment. For example, gap junctions close in the presence of high intracellular Ca^{2+} or low pH, which requires elevating the J from a constant to a function of the local chemical gradient $C(x,t)$

$$J \to J_{ij}(C) \tag{8}$$

If a tumor microenvironment becomes highly hypoxic and acidic, $J \to 0$. The local biological units decouple from the systemic homeostatic network (the system loses its long-range correlation length, ξ), allowing the pathology to establish its own isolated, rigid phase.

Combining these aspects, the unified extended Hamiltonian for the biological system is:

$$\mathcal{H}_{total} = -\sum_{\langle i,j \rangle} J_{ij}(C) s_i s_j - \sum_i \left(\left(h_{thermal} + \mu_c + \gamma_i E_{nT}(t) \right) n_i \right) \tag{9}$$

The partition function Z, which now sums over all microstates while accounting for both thermal noise ($\beta = \frac{1}{k_B T}$) and chemical/nonthermal energetic shifts, becomes:

$$Z_{total} = \sum_{\{s\}} \exp\left(-\frac{\mathcal{H}_{total}}{k_B T} \right) \tag{10}$$

By rewriting the model this way, we encode, rather than prove the hypothesis that a targeted nonthermal interventions can shift the system's energy minimum; whether real interventions realize this shift is a testable prediction. If a pathological tissue has decoupled itself chemically ($J \to 0$) and established a highly ordered, rigid state ($m \to 1$), simply raising the systemic temperature (T) may not be enough to break its equilibrium before damaging healthy tissue.

2.3. Biological Mapping Strategies

Mapping real biological systems onto the Ising framework requires identifying the relevant "spins" and "couplings". In neural networks, spins correspond to the binary firing states of neurons (active/silent), and couplings encode synaptic strengths. In gene regulatory networks, spins represent the on/off expression states of genes, with couplings derived from transcription factor binding affinities. At the cellular scale, particularly relevant to cancer and tissue biology, spins map onto cell phenotypic states (proliferative/quiescent, epithelial/ mesenchymal), and couplings represent cell-cell signaling, adhesion, and mechanical interactions.

A particularly powerful approach is the maximum entropy framework [36], in which the Ising couplings J_{ij} and local fields h_i are inferred directly from experimental data (e.g., multi-electrode recordings, single-cell RNA-seq, or calcium imaging) by requiring that the model reproduce the observed first and second moments of the data, the mean activities $\langle s_i \rangle$ and pairwise correlations $\langle s_i s_j \rangle$, with maximum entropy (minimum assumptions) otherwise. This inverse

Ising problem has been solved using mean-field approximations [37], belief propagation [38], and Monte Carlo methods [39].

2.4. $1/f$ Noise as a Signature of Self-Organized Criticality in Biology

A signal $x(t)$ is said to exhibit $1/f$ noise (pink noise) when its power spectral density $S(f)$ scales as:

$$S(f) \propto \frac{1}{f^{\alpha}} \quad 0.5 \le \alpha \le 1.5 \quad (\text{pink or } 1/f \text{ noise when } \alpha \approx 1) \tag{11}$$

In the Ising framework, the connection between criticality and $1/f$ dynamics arises from the divergence of the autocorrelation time $\tau \propto \xi^{z}$ (where z is the dynamical exponent) as the correlation length $\xi \to \infty$ at the critical point. The resulting superposition of exponentially decaying correlations over all time scales, weighted by the critical distribution of cluster sizes, generates the $1/f$ spectrum. This is a rigorous result within the theory of critical slowing-down and applies broadly to all systems near a second-order phase transition.

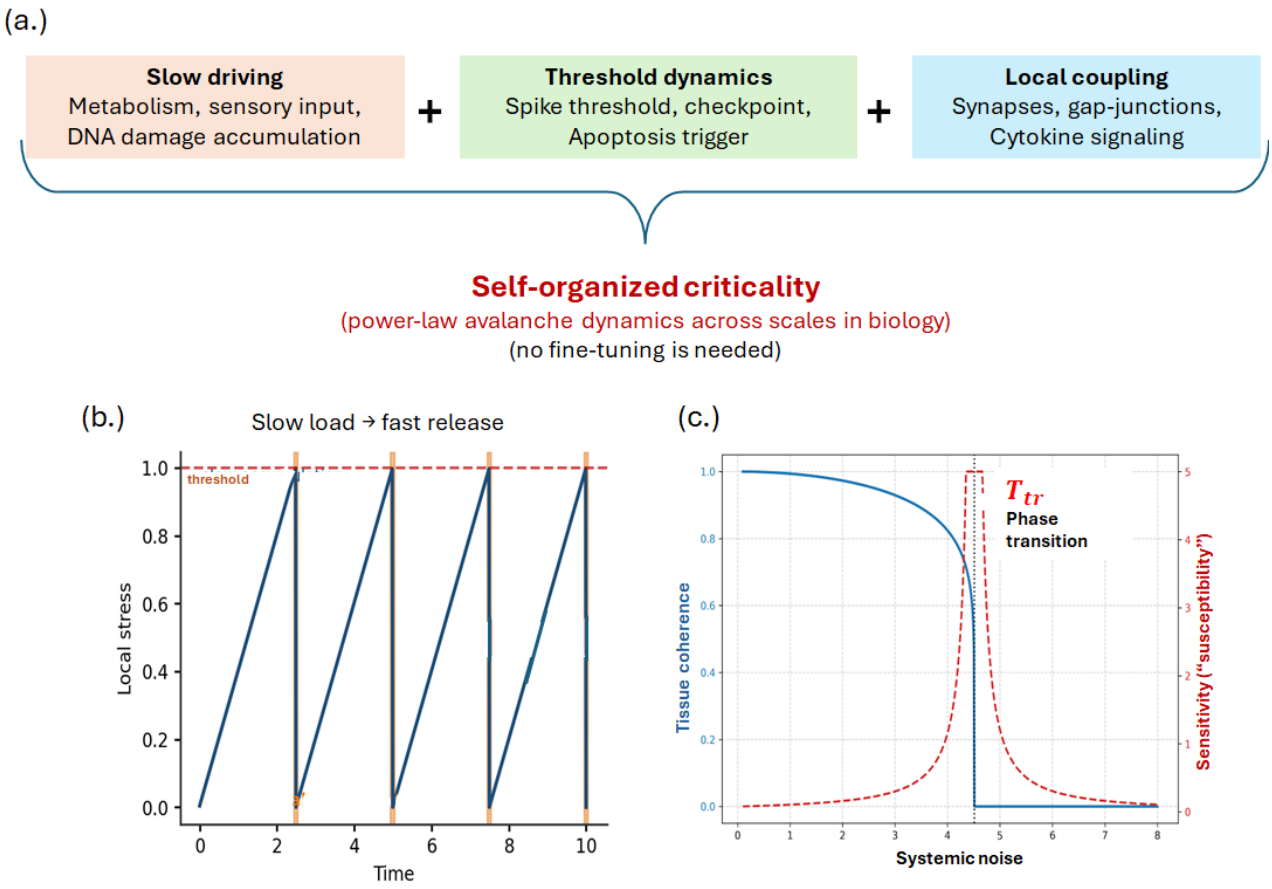

Figure 2. Self-organized criticality (SOC) in biosystems. (a) The three-ingredient recipe for SOC in homeostatic control: slow driving + threshold + local coupling → criticality. (b) The typical SOC process is homeostatic control: slow loading and fast release (avalanche-like phenomena) when the threshold is reached. (c) Criticality and phase transition in homeostasis. Tissue coherence abruptly drops at the transition temperature, while sensitivity and other physical parameters increase significantly.

A crucial theoretical question is why biological systems would be poised near criticality. Evolutionary selection may favor criticality because it maximizes computational capacity: critical systems exhibit the longest memory, the greatest sensitivity to inputs, and the richest repertoire of dynamical states, properties that confer adaptive advantages.

The complexity of living systems is in a critical stage, developing self-organized criticality (SOC) [40], which is formulated as the "life at the edge of chaos" [41]. The permanent control of homeostatic equilibrium and the opposing effects of the balancing factors indicate the "edge of chaos" [25]. It provides a dynamical mechanism by which systems with slow driving and fast relaxation spontaneously evolve toward the critical state without fine-tuning of parameters (**Figure 2**). It predicts that systems driven slowly with local dissipation, sandpiles, earthquakes, forest fires, and neural networks, will self-organize to the critical point, and that the resulting dynamics will exhibit $1/f$ power spectra and power-law size distributions of "avalanches". While $1/f$ spectra are consistent with critical dynamics, they may arise from alternative mechanisms such as superposed relaxation processes.

2.5. Homeostasis as Criticality: The Healthy Organism at the Edge

However, by tuning the non-thermal field $E_{nT}(t)$ to match the specific susceptibility γ_i of the diseased state, you apply a targeted energetic penalty that forces the local Hamiltonian into an unstable state, catalyzing a localized phase transition back toward systemic control.

This paradox of a homeostatic equilibrium and ever-changing dynamism, and the critical stage at the edge of chaos and order, is resolved by the critical state hypothesis: healthy physiology operates near a critical point, generating $1/f$ noise and power-law statistics that reflect the long-range temporal correlations of a system near criticality. The Ising analogy is instructive: a ferromagnet precisely at critical temperature (T_c) displays fluctuations at all spatial and temporal scales simultaneously; it is neither rigid (ordered) nor incoherent (disordered). Healthy tissue in this model occupies an analogous position in its own phase space.

The multicellular organism can be viewed as a vast network of coupled oscillators and binary-state decision-makers, embedded in a noisy thermal-like environment. Gap junctions, paracrine signaling molecules, mechanical stress transmission through the extracellular matrix, and electrical field coupling all provide the physical substrate for Ising-like interactions between cells. The state of a cell at any moment reflects the integrated outcome of these interactions and its internal signaling state.

In healthy tissue, these couplings maintain the critical balance between local order (domain formation, coordinated cell behavior) and global disorder (independence, heterogeneity). The correlation length is large but finite, communication propagates across many cell diameters, enabling coordinated responses to perturbation without catastrophic, system-wide phase transitions that would

compromise function. The system retains both sensitivity (to respond to growth factor gradients, injury signals, or metabolic needs) and stability (to resist runaway proliferation or excessive apoptosis).

The Ising model also provides a natural language for developmental processes. Embryogenesis requires the symmetry-breaking passage from a uniform, undifferentiated state (analogous to the high-temperature disordered phase) to spatially organized, differentiated tissue (analogous to the ordered, magnetized phase). Reaction-diffusion systems, morphogen gradients, and cell fate decision circuits can all be analyzed as systems undergoing effective phase transitions, with the critical point corresponding to bifurcations in the underlying dynamical systems. Epigenetic landscapes, as formalized by Waddington, can be reinterpreted as free-energy surfaces within a statistical-mechanical framework, with cell differentiation as a descent into energy minima separated by saddle points, traversed near criticality.

3. Loss of $1/f$ Complexity

The most clinically striking feature of $1/f$ noise in physiology is its systematic degradation in aging and disease. It was documented [42] extensively that: (1) normal sinus rhythm exhibits $1/f$ HRV scaling; (2) aging progressively reduces the exponent α toward white noise ($\alpha \to 0$, loss of long-range correlations, loss of criticality); (3) pathological states, congestive heart failure, diabetic autonomic neuropathy, atrial fibrillation, Alzheimer's disease, shift HRV spectra either toward white noise (excessive disorder) or toward sinusoidal regularity (excessive order), both representing departures from the critical intermediate.

This bidirectional loss of complexity, the complexity loss theory of disease and aging [43], maps precisely onto the biophysical picture of departure from criticality. In the Ising analogy, the aging or diseased organism shifts away from the critical point T_{tr} either toward the ordered phase ($T_{eff} < T_{tr}$: rigid, stereotyped dynamics, excessive correlations) or toward the disordered phase ($T_{eff} > T_{tr}$: random, uncorrelated fluctuations, failure of coordination). Both trajectories are pathological.

Crucially, $1/f$ exponent analysis (detrended fluctuation analysis, DFA; or multi-scale entropy, MSE) of physiological time series has emerged as a practical clinical tool. DFA scaling exponents of HRV, gait variability, and EEG distinguish healthy controls from at-risk patients, with sensitivities and specificities competitive with or exceeding those of conventional biomarkers. The DFA exponent is, in effect, a quantitative measure of how close a physiological system is to its critical point.

Cancer cells and tumor tissue exhibit profound alterations in $1/f$ noise characteristics. At the membrane level, the ion channel current fluctuations of cancer cells show altered $1/f$ exponents relative to their normal counterparts, reflecting the disrupted lipid-raft criticality. Patch-clamp recordings from cancer cell lines consistently show power spectra that deviate from the near-unity α of normal

epithelial cells, shifting toward either $\alpha < 0.5$ (excessive randomness) or $\alpha > 1.5$ (excessive slow fluctuations indicative of anomalous diffusion in altered membrane environments).

At the network level, the electrical impedance spectra of tumor tissue (measurable non-invasively by bioimpedance spectroscopy) show characteristic deviations from the Cole-Cole model with $1/f$ exponents altered relative to normal tissue. These spectral alterations are directly exploited in bioimpedance-guided targeting used in mEHT systems, providing a biophysical rationale for selective energy deposition in tumor versus normal tissue [44].

Signs of criticality are observed in neural systems and in homeostatic plasticity mechanisms, in which neurons regulate their own excitability and synaptic strengths to maintain a target mean firing rate, have been shown theoretically and experimentally to drive networks toward critical branching ratios. In neural networks, the prediction is neuronal avalanches whose size distribution $P(s) \propto s^{-3/2}$ and duration distribution $P(t) \propto t^{-2}$, precisely the mean-field critical exponents [31] confirmed these predictions in cortical slices, and subsequent in vivo studies have extended these findings across species and brain regions.

The dynamical fractal structure marks the self-organization both in structural and time arrangements [40], and it dynamically regulates the living matter [45]. The $1/f$ fluctuations [12] define the time-fractal structure of living systems in a stochastic manner [11]. The self-similarity gives a scale-free structure of $1/f$, so that each octave interval (halving or doubling in frequency) carries an equal amount of noise energy in the $1/f$ noise. Aging and diseases modify the noise spectrum, with a gradual loss of system complexity (**Figure 3**).

The healing mechanism restores homeostatic control, keeping the system at maximum sensitivity and adaptability. The self-organized geometric network symmetry of living systems can transform the white noise into pink noise [46], forming the most common signal in biological systems [47].

The long-range memory of $1/f$ noise ensures that distant parts of a tissue, or different regulatory loops, remain coupled. It is the hallmark of SOC when the system is constantly communicating with itself across all times and spatial scales to stay at the "edge of chaos." This chaos is the realization of a well-organized stochastic (probabilistic) system [48]. Chaos is only an ostensible complete disorder [49].

Modeling such a complex system as biological homeostasis is challenging. Usually, only a few key critical behaviors of these systems can be accurately described and mathematically analyzed. One of these critical structures the self-organized criticality describes the living dynamism as the edge of chaos and order, calculating a second-order phase transition that characterizes that "edge", the homeostatic dynamic equilibrium. Such a mathematically manageable, statistically correct model is the Ising model.

At SOC, the system may be poised at a critical state at the boundary between distinct dynamical regimes. The self-organization of living systems towards crit-

icality leads to a pure $1/f$ spectrum [40]. The criticality may have been evolutionarily selected [50]. A precise $1/f$ noise was found for optimum growth and for the physiological ("healthy") state of human blood cells, where the temperature-driven dynamics select the exact exponent of the frequency as -1 at healthy human body temperature with a sharp Lorenz peak [51]. The $1/f$ spectrum was observed in numerous biological systems [52]. These give strong support for the chosen $1/f$ spectra for modulation in α-dispersion range [53] [54].

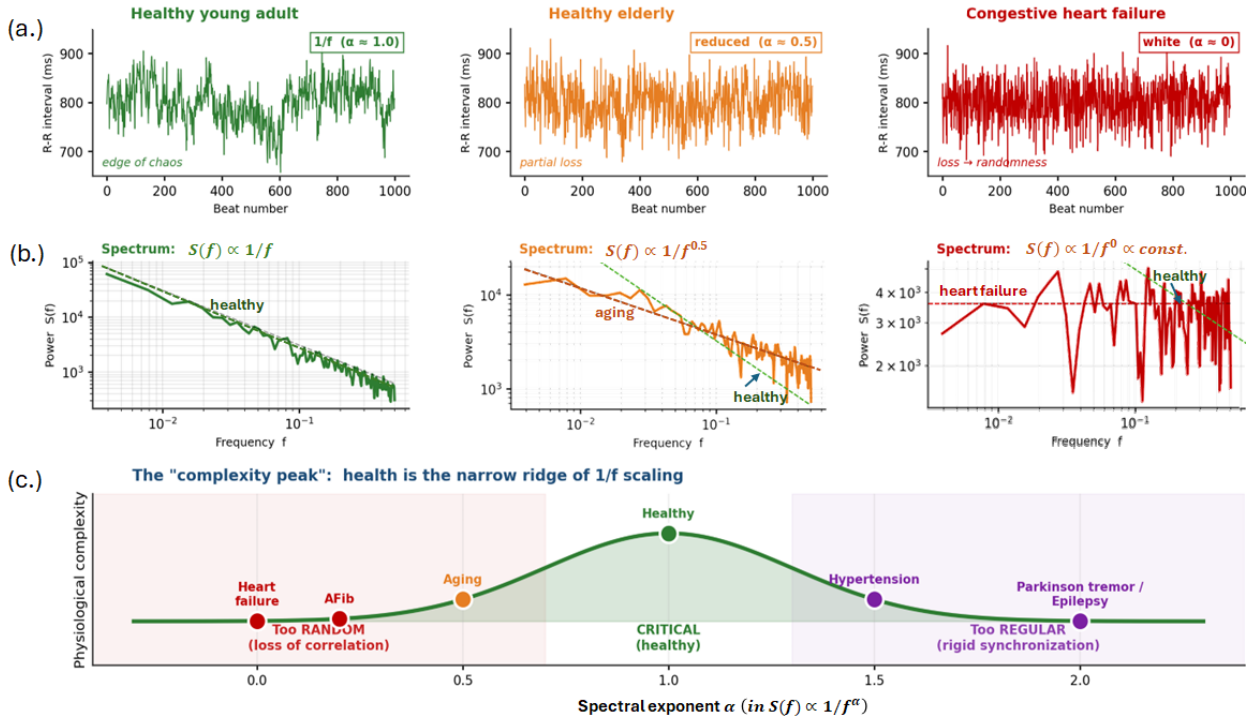

Figure 3. Loss of complexity. Aging and disease shift the equilibrium from the edge. (a) The noises of the stages. (b) the frequency distribution. (c) Complexity is lost when leaving the homeostatic peak. The complexity peak locates various pathologies along the α axis, heart failure and AFib on the random side, hypertension and Parkinsonian tremor on the over-regular side, with the narrow ridge of health at $\alpha \approx 1$. (The figure shows real-looking HRV signals and their power spectra for healthy young adults ($1/f$), elderly (reduced exponent), and CHF (white noise)).

Traditional physiology defined health as the maintenance of stable, constant internal conditions, inspired by Claude Bernard's milieu interior [55], Walter Cannon's homeostasis [56]. However, a closer look at healthy physiological signals shows that stability is not the defining feature of health; instead, it is structured variability. Heart rate variability (HRV), respiratory rate, electroencephalographic (EEG) oscillations, and gait fluctuations all demonstrate non-stationary, scale-free dynamics in healthy individuals, and a shift toward regularity or randomness in disease and aging.

3.1. Oncogenesis as a Departure from Criticality

Cancer is, at its core, a disease of disrupted cellular cooperation. Malignant transformation involves not merely the autonomous dysregulation of individual

cells but the breakdown of the cooperative tissue-level order that normally constrains proliferation and maintains differentiation. From the perspective of the Ising model, oncogenesis can be conceptualized as a phase transition away from the critical regime, either toward excessive order (clonal dominance, synchronized oscillations in metabolic states) or toward excessive disorder (genomic instability, phenotypic heterogeneity, loss of coordinated signaling). Very near to the breaking of criticality, the critical exponents define the deviation.

The tumor microenvironment (TME) presents a profoundly altered physical and chemical milieu: hypoxic gradients, acidification, elevated interstitial pressure, and remodeled extracellular matrix all alter the effective "temperature" and "coupling constants" of the cellular Ising system. Tumor cells frequently exhibit altered gap junction composition, reduced connexin expression, and dysregulated paracrine signaling, effectively decoupling them from the cooperative network. This decoupling shifts the effective J and T parameters of the tissue Ising model, moving the system away from criticality.

3.2. Membrane Phase Separation and Lipid Raft Dynamics

A particularly compelling application of Ising criticality in oncology concerns the plasma membrane. The biological cell membrane is a two-dimensional fluid bilayer composed of hundreds of lipid species, cholesterol, and embedded proteins, and it is a realization of a 2D Ising universality class system. The lipid vesicle membranes composed of ternary lipid mixtures exhibit a miscibility critical point whose universality class matches that of the 2D Ising model, characterized by critical fluctuations between liquid-ordered (L_o) and liquid-disordered (L_d) phases [57].

Critically, plasma membrane compositions of living cells appear to be poised near this miscibility critical point at physiological temperatures. Critical fluctuations in membrane composition give rise to the transient, nanoscale lipid raft domains that organize signaling receptors, regulate receptor-ligand binding kinetics, and modulate the lateral diffusion of membrane proteins. In cancer cells, altered lipid metabolism (increased cholesterol, modified fatty acid saturation profiles) shifts the membrane away from criticality, disrupting raft dynamics and altering the spatial organization of receptor tyrosine kinases, G-protein coupled receptors, and immune checkpoint molecules.

Altered lipid raft dynamics in cancer cells affect EGFR dimerization, RAS clustering, and PD-L1 distribution, providing mechanistic links between membrane biophysics, oncogenic signaling, and immunotherapy response. Restoring membrane criticality may therefore be a novel therapeutic target. This is recognized and used by modulated electrohyperthermia (mEHT).

3.3. Epithelia-Mesenchymal Transition as a Phase Transition

The epithelial-mesenchymal transition (EMT), a process by which epithelial cells acquire mesenchymal, invasive characteristics central to metastasis, can be for-

malized as a first-order phase transition in a multi-stable genetic regulatory network. The core EMT regulatory circuit, involving mutual inhibition between the epithelial transcription factor CDH1 (E-cadherin) and the mesenchymal factors SNAIL, TWIST, and ZEB, constitutes an effective bistable Ising-like spin system at the cellular level. The transition between states is driven by TME signals that function as an effective external field h, tilting the effective free energy landscape. Near the transition, cells traverse a hybrid E/M state that displays maximal phenotypic plasticity, an analog of the critical fluctuations of the Ising model.

4. Tumor Heterogeneity and Spin Glass Dynamics

The remarkable phenotypic heterogeneity of solid tumors, in which cells from the same lesion display dramatically different gene expression profiles, metabolic states, and drug sensitivities, is naturally accommodated by a spin glass generalization of the Ising model. In spin glass systems, the coupling constants J_{ij} are random variables, drawn from a distribution with zero mean and finite variance. The resulting frustrated interactions lead to an exponentially large number of metastable states (a complex free-energy landscape with many local minima), slow relaxation dynamics, and extreme sensitivity to initial conditions, all hallmarks of tumor biology.

Tumor cells embedded in a heterogeneous microenvironment, with randomly varying paracrine signals, matrix stiffness gradients, and oxygen partial pressures, experience precisely such frustrated, disordered coupling. The spin glass framework predicts the coexistence of multiple cellular phenotypes, the dynamic interconversion between states driven by stochastic fluctuations, and the difficulty of therapeutic targeting (analogous to the hardness of finding the ground state of a spin glass, an NP-hard computational problem).

While the Ising model and its lattice-gas variants are excellent for modeling phase transitions in cooperative, homogeneous biological networks, they often fall short in describing the messy, conflicting reality of complex pathologies. This is where the spin-glass model becomes a vital biophysical tool.

If the Ising model represents a healthy, unified tissue acting in cooperative synchrony, the spin-glass model represents the chaotic, deeply entrenched, and highly resistant state of a pathological network, such as a tumor microenvironment (TME).

The fundamental difference between the two models lies in the nature of intercellular coupling:

1) In the standard Ising model (cooperative homeostasis) the coupling constants are uniform and positive ($J_{ij} > 0$). Every discrete unit (cell) seeks to align its state with its neighbors. This provides a model of healthy tissue that has intact gap junctions and paracrine signaling. The cells cooperate to maintain a unified homeostatic state, easily sharing resources and electrical polarization.

2) In the spin-glass model (pathological frustration), the couplings (J_{ij}) are

drawn from a random probability distribution containing both positive (cooperative) and negative (antagonistic) interactions. This creates frustration: a state in which a cell cannot simultaneously satisfy the conflicting demands of all its neighbors. In a TME, signaling is highly dysregulated. Hypoxia, necrotic cores, and erratic vascularization create conflicting chemical gradients. Some cells emit pro-survival signals while neighboring immune cells or hypoxic stressors emit pro-apoptotic signals. The tissue is functionally "frustrated," unable to find a simple, unified consensus.

4.1. The Energy Landscape and Metastability

The nature of the interactions defines the Hamiltonian ($\mathcal{H}$) and drastically alters the thermodynamic energy landscape of the tissue (Figure 4).

1) Ising energy landscape (smooth and symmetrical) is relatively smooth, resembling a wide valley with one or two deep, global minima (e.g., completely healthy or completely apoptotic). Below the critical temperature (T_c), the system effortlessly settles into a highly ordered global minimum.

2) Spin-glass landscape (rugged and ultrametric) because of frustration. The spin-glass energy landscape is extraordinarily "rugged," filled with countless local valleys, ridges, and metastable minima. This perfectly describes the resilience of malignant homeostasis. A tumor does not represent a true global equilibrium; it is trapped in a sub-optimal, rigid, metastable state. Because the energy barriers between these local valleys are so high, normal systemic fluctuations (healthy biological noise) are entirely insufficient to dislodge the malignant tissue from its pathological route.

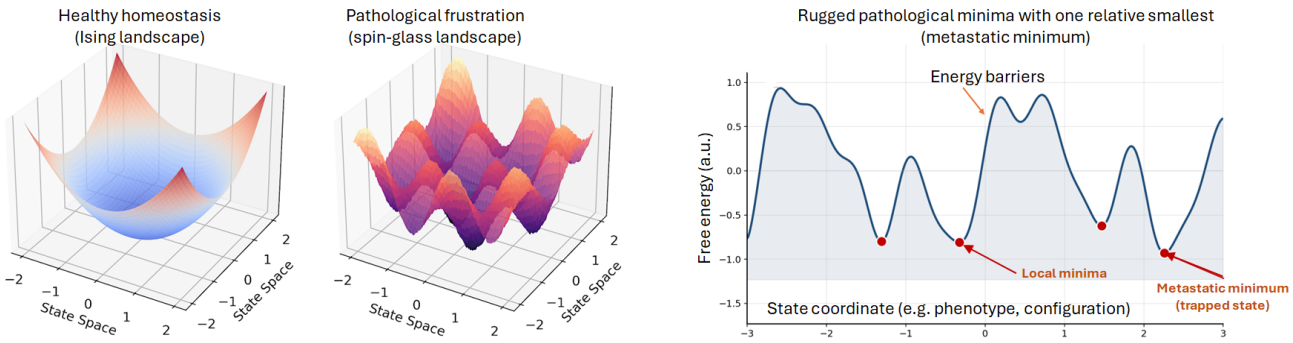

Figure 4. The models of the healthy and pathological states. (a) Healthy homeostasis is characterized by a definite energy minimum, modeled using the Ising process. (b) The pathological state has a rugged landscape with multiple minima. (c) The free energy in a one-dimensional state coordinate shows the relative lowest minimum, when the system could be trapped, while locally also blocked in wells, from where the escape is to the lower minima.

4.2. Response to External Interventions (Bulk vs. Modulated Energy)

This thermodynamic comparison explains why simply heating a tumor (classic hyperthermia) often fails, and why modulated, non-thermal targeting is required.

1) Perturbing the Ising model with a uniform external field $\mathbf{h}$ or a bulk temperature increase (T) easily tilts the smooth energy landscape, forcing the cooperative cells to flip into a new phase.

2) Perturbing the spin-glass model with a uniform field (like bulk, unmodulated heat) to a spin-glass merely "jiggles" the system within its rugged local valley. Because the interactions are frustrating and heterogeneous, bulk energy does not provide a coherent direction for the tissue to follow. To break a spin-glass state, one must apply a specific, time-dependent, modulated field that couples directly to the unique susceptibilities (γ_i) of the trapped nodes. By targeting the specific dielectric properties of the malignant cells, the intervention selectively lowers the energy barriers of the rugged landscape, forcing the trapped system to "melt" and reorganize, allowing the broader, healthy homeostatic field to clear the pathology.

To mathematically capture a biological reality in which a highly ordered, healthy system, a frustrated tumor core, and an actively hostile immune boundary coexist, we must abandon the assumption of a globally homogeneous coupling distribution. Instead, we must define the coupling distribution $P\left(J_{ij}\right)$ as a spatially structured, multi-phase distribution. By compartmentalizing the network, we can model the tissue as a set of distinct thermodynamic "players," effectively framing the cellular interactions as a localized game-theoretic equilibrium, and formulate the topologically dependent coupling distribution.

4.3. Defining the Topological Compartments

Let us assign every discrete cellular node i to a specific biological subset based on its spatial coordinate r_i:

V_H (healthy tissue), assigns the surrounding host bulk tissue, maintaining regular homeostatic order. V_T (tumor core) corresponds to the hypoxic, dysregulated, usually necrotic glassy core, V_I (immune infiltrate) designed for the boundary layer or infiltrating immune cells acting at the interface of V_H and V_T.

We can define the overarching coupling distribution as a spatial mixture model, where the nature of J_{ij} depends entirely on the identities of the interacting pair:

$$P\left(J_{ij}\right)=\sum_{\alpha,\beta\in\{H,T,I\}}\delta\left(i\in V_\alpha\right)\delta\left(j\in V_\beta\right)P_{\alpha\beta}\left(J_{ij}\right) \tag{12}$$

where δ is the Dirac delta (or a Kronecker delta for discrete sets), ensuring that the correct sub-distribution $P_{\alpha\beta}$ is applied to the edge connecting node i and node j.

The sub-distributions ($P_{\alpha\beta}$) has localized groups as healthy-healthy (P_{HH}), tumor-tumor (P_{TT}) and active boundary (immune-tumor) (P_{IT}) factions. Let's suppose that each localized distribution is a Gaussian $\aleph\left(x,\mu,\sigma^2\right)=\frac{1}{\sigma\sqrt{2\pi}}\exp\left(-\frac{1}{2}\left(\frac{x-\mu}{\sigma}\right)^2\right)$, but with vastly different means and

variances to represent the local biological physics.

The homeostatic bulk P_{HH} has strong, positive "ferromagnetic" coupling. The low variance ensures that almost all interactions are cooperative, yielding the long-range correlation lengths ($\xi \to \infty$) and $1/f$ noise characteristic of robust systemic regulation. In these conditions:

$$J_{ij} \propto \aleph\left(J_0, \sigma_H^2\right) \text{ where } J_0 > 0 \text{ and } \sigma_H \ll J_0 \tag{13}$$

The rugged core (tumor-tumor, P_{TT}) can be modeled with the classic spin-glass [58], where the mean coupling is zero, but the variance is massive. The tissue is deeply frustrated by conflicting signals (hypoxia, chaotic angiogenesis), trapping the core in a rigid, localized, and highly stable sub-optimal equilibrium

$$J_{ij} \propto \aleph\left(0, \sigma_T^2\right) \text{ where } \sigma_T \text{ is large} \tag{14}$$

The active boundary (immune-tumor P_{IT}) is a strong "antiferromagnetic" (antagonistic) interaction. The immune cells (V_I) are actively attempting to flip the state of the malignant cells (V_T) toward apoptosis. This creates a massive thermodynamic "surface tension" at the tumor boundary.

$$J_{ij} \propto \aleph\left(-J_{ant}, \sigma_{IT}^2\right) \text{ where } J_{ant} > 0 \tag{15}$$

4.4. The Game-Theoretic Stalemate and Its Braking

By defining $P\left(J_{ij}\right)$ this way, the Hamiltonian reveals why natural immune clearance often fails. At the boundary, the immune cells deploy a highly antagonistic "strategy" ($-J_{ant}$). However, because the tumor core (V_T) is bound by the rugged spin-glass matrix (σ_T^2), the energy required to flip a single tumor cell is extremely high. The tumor's glassy metastability acts as a defensive Nash equilibrium, where the change from any antagonistic sides makes worst payoff, so this is the local equilibrium. The immune cells can push against the boundary, but the perturbation cannot propagate into the core because the spin-glass lacks the necessary correlation length to carry the signal. The system is locked in a frustrated stalemate.

The grand canonical Hamiltonian with the non-thermal intervention term (Equation (9)) can break this stalemate Nash equilibrium:

$$\mathcal{H}_{total} = -\sum_{\langle i,j \rangle} J_{ij} s_i s_j - \sum_i \left(\mu_c + \gamma_i E_{nT}\left(t\right)\right) n_i \tag{16}$$

When a highly targeted, modulated intervention (like mEHT) is applied, the field $E_{nT}\left(t\right)$ couples exclusively to the high susceptibility (γ_i) of the V_T nodes. The electric field of mEHT forcefully elevates the local energy state of the tumor nodes. This "melts" the rugged landscape of P_{TT}, effectively erasing the high variance σ_T^2 that was protecting the core. With the core's defensive equilibrium disrupted, the strong antagonistic coupling from the immune boundary (P_{IT}) rapidly cascades inward, driving a phase transition that collapses the malignant network and further drives it toward the immunogenic solution, the strong part of mEHT (see later).

4.5. The Critical Values at the Edge of Chaos

The three-dimensional (3D) models of biological tissues are spatial networks that need to accurately compare the numerical values of the critical temperature (T_c) and critical exponents.

For the standard Ising model, we assume a 3D simple cubic lattice with uniform ferromagnetic coupling ($J > 0$). For the spin-glass model, we use the 3D model [58] with a Gaussian distribution of couplings ($\mu = 0$, $\sigma^2 = J^2$).

It is important to note that while the 3D Ising exponents are known to extremely high precision via conformal bootstrap and renormalization group methods. 3D spin-glass exponents are notoriously difficult to calculate and are derived primarily from massive Monte Carlo simulations, leading to slight numerical uncertainties.

The stark contrast in the numerical values (**Table 2**) provides the strict thermodynamic justification for why malignant tissues behave differently than healthy tissues, and why standard interventions often fail. There is a drastic drop in critical temperature (T_c/T_g), the spin-glass transition occurs at a radically lower "temperature" (systemic noise level) than the Ising transition. This is because of the deep frustration (conflicting signaling, hypoxia) in the tumor core, the tissue cannot maintain a highly ordered state at normal physiological noise levels. It "freezes" into its rigid, sub-optimal pathological state at a much lower threshold. The tumor is thermodynamically isolated from the higher-energy cooperative dynamics of the surrounding healthy tissue.

The massive shift in susceptibility (γ) is observed. In the Ising model, standard linear susceptibility diverges, in a spin-glass, linear susceptibility (χ) does not diverge at all (it merely forms a cusp). Instead, it is the non-linear susceptibility (χ_{NL}) that diverges, and it does so with a massive exponent. This is perhaps the most critical mathematical distinction for therapeutic intervention. The spin-glass tumor core responds only weakly to a linear, bulk physical force (such as standard, unmodulated macroscopic heating) because its linear susceptibility exhibits only cusp-like behavior, whereas higher-order nonlinear susceptibilities diverge strongly. However, because χ_{NL} diverges with an enormous exponent near T_g. The tumor core is mathematically hypersensitive to nonlinear, time-varying interventions (such as specific amplitude-modulated electromagnetic fields). The divergence of the nonlinear susceptibility suggests a route by which a modulated intervention could couple more strongly to the frustrated spin-glass core than to the cooperative Ising-like tissue (which lacks divergence). This is a model-based expectation rather than a proof: the degree of selectivity in tissue must be established experimentally, and healthy tissue is expected to be less affected.

The spin-glass has a negative specific heat exponent while the 3D Ising model has a small positive α. The specific heat sharply diverges (a sharp phase transition) in the spin-glass α is highly negative. A negative α means the specific heat does not approach infinity at T_g; the phase transition is incredibly

"smeared out" or sluggish h. The tumor does not abruptly collapse when systemic conditions change; its frustrating nature allows it to absorb thermal energy through countless metastable pathways without actually changing its fundamental biological state.

The dynamic relaxation (z) diverges. The dynamical critical exponent z dictates the relaxation time ($\tau \propto \xi^2$). In the spin-glass, z is roughly three times larger than in the Ising model. When a healthy tissue (Ising) is perturbed, it recovers its homeostatic equilibrium relatively quickly. When a glassy tumor core is perturbed, its relaxation time is astronomically long. If you apply a pulsed or modulated non-thermal field at a frequency that is faster than this deeply sluggish relaxation time, the malignant tissue cannot dissipate the absorbed energy through normal homeostatic pathways. The energy accumulates explicitly in the pathological network, forcing the localized transition into apoptosis.

Table 2. The numerical comparison and what these profound differences mean for biophysics and targeted interventions.

Parameter/Exponent	2D Ising model	3D Ising model (Healthy homeostasis)	3D Spin-Glass (Pathological core)	Mathematical/Physical definition
Critical Temperatures (T_c/ T_g)	$\frac{k_B T_c}{J} \cong 2.27$	$\frac{k_B T_c}{J} \cong 4.51$	$\frac{k_B T_g}{J} \cong 0.95$	The noise threshold where the phase transition occurs.
α (Specific heat)	0	≈0.110	≈-1.5 to -2.0	Divergence of heat capacity (energy fluctuations).
β (Order parameter)	1/8	≈0.326	≈0.7 to 0.8	Scaling of magnetization (m) vs. Edwards-Anderson overlap (q).
γ (Susceptibility)	7/4	≈1.237 (linear χ)	≈5.5 to 6.5 (nonlinear χ_{NL})	Responsiveness of the system to an external field.
ν (Correlation length)	1	≈0.630	≈2.4 to 2.8	How rapidly the influence of one cell spreads to others.
z (Dynamical)	≈2.17	≈2.02	≈5.5 to 6.5	"Critical slowing down" (relaxation time recovery).

5. Principles of mEHT

Modulated electro-hyperthermia (mEHT, commercially known as oncothermia) is a cancer treatment modality [59] that applies amplitude-modulated radiofrequency (RF) electromagnetic fields, typically at 13.56 MHz, with complex modulation signatures that include components spanning a broad frequency range, including the $1/f$ noise regime, to tumor tissue [53] [54]. Unlike conventional whole-body or regional hyperthermia, which aims primarily for uniform thermal elevation, mEHT exploits the dielectric and electrical properties of tumor tissue to achieve preferential energy deposition in the tumor relative to surrounding normal tissue and to induce non-thermal effects at the cellular and subcellular scales.

The key biophysical principle underlying mEHT's selectivity is the differential dielectric properties of tumor versus normal tissue [60] [61]. mEHT likely acts through a combination of dielectric selectivity, membrane-level nonlinearities, and network-level critical dynamics. Tumor membranes, with their altered lipid compositions, elevated membrane cholesterol, and dysregulated ion channel expression, exhibit distinct complex permittivity spectra $\varepsilon^*(\omega)=\varepsilon'(\omega)-i\varepsilon''(\omega)/\omega$ relative to normal tissue. The β-dispersion of tissue dielectric properties (occurring in the MHz frequency range, arising from Maxwell-Wagner polarization at cell membrane interfaces, β-dispersion) is particularly relevant: it governs the fraction of applied RF energy absorbed at membrane interfaces versus intracellular space [62]. The RF current exhibits a characteristic dispersion in the MHz frequency range (upper β-dispersion [63], which referred in the literature as δ-dispersion [64] and the Schwan effect [35]), which highlights lipid–protein interactions and selects water-bound states [65] at the membrane, effectively directing energy to the target [66].

The mEHT applies a frequency at the high end of this special frequency range (δ-dispersion) using 13.56 MHz, an ISM-band frequency allocated for industrial, scientific, and medical use. The high-frequency β/δ dispersion selects the malignant cells and promotes energy absorption in their membrane rafts. The targeted rafts influence transport and signal transduction [67], are involved in numerous signal paths, and sense various stresses [68]. However, the application of low frequency (α-dispersion) would be essential for triggering the necessary homeostatic and intracellular signals. The mEHT resolves the apparent contradiction of simultaneously having a high selection frequency and a low homeostatic $1/f$ spectrum, involving the transmembrane protein excitations. The solution to the challenge is that the appropriate low-frequency amplitude modulates the high-frequency carrier. The membrane rectifies the modulated signal. The carrier frequency in the rectified signal remains active, but mainly at the cellular membrane. In this way, the original modulation signal drives the excitation process. The amplitude-modulation results demonstrate the concept [41].

5.1. Membrane Targeting and Ising Criticality

The most important non-thermal mechanism of mEHT, from a biophysical standpoint, is its action on membrane lipid raft dynamics. The oscillating electric field at 13.56 MHz directly couples to the dipolar and ionic constituents of the membrane bilayer, driving oscillations in lipid domain boundaries. The raft arrangement in the healthy membranes can be described with 2D Ising model [69], having curvature stabilization [70]. The membrane-raft coexistence structure can be described with two interacting 2D layers [71]. At criticality, lipid domain fluctuations are maximally sensitive to external perturbation, and so the dielectric susceptibility χ is at its maximum (in principle infinite).

In tumor cells, the departure from membrane criticality reduces this susceptibility, but simultaneously creates large-scale compositional inhomogeneities (phase-

separated domains rather than critical fluctuations). The amplitude-modulated RF field of mEHT preferentially couples to these inhomogeneous domains through their enhanced local dielectric contrast, depositing energy selectively at domain boundaries [72], the analog of domain walls in an Ising ferromagnet. Domain wall dynamics in 2D Ising systems are known to exhibit rich nonlinear behavior, including roughening transitions and critical slowing-down phenomena, which translate in the biological context to disruption of raft-associated signaling complex assembly.

5.2. The $1/f$ Modulation Spectrum and Biological Resonance

A defining feature of mEHT, distinguishing it from conventional RF hyperthermia, is its complex amplitude modulation pattern. The modulation signal contains components across a broad frequency band, with a power spectral density approximating a $1/f$ (pink noise) spectrum in the low-frequency range (0.1 - 100 Hz). This feature is not merely a technical artifact but a deliberate design choice with deep biophysical rationale.

As elaborated above, healthy biological systems generate $1/f$ noise as a hallmark of their operation near criticality [40]. Biological oscillators, including membrane potential fluctuations, cytoskeletal dynamics, and metabolic oscillations, are entrained to and resonate with $1/f$-distributed inputs. The application of $1/f$-modulated electromagnetic fields can therefore be understood as providing a stochastic resonance (SR) input that preferentially engages systems operating in the critical regime. Healthy cells, operating near criticality, respond adaptively to this input (with possible beneficial effects on gap-junction communication and stress-response coordination), while tumor cells, shifted away from criticality into a disordered or spin-glass-like regime, experience destructive interference between the applied field and their dysregulated intrinsic dynamics. The nonthermal effects do not attributable to a rise in bulk temperature, but it is not the absence of any heating; the modulation supplies a directed bias while the carrier supplies stochastic drive. The thermal component significantly influences reaction conditions and speed (Arrhenius effect), making the thermal background essential for optimizing the mEHT effect.

In the point of healthy homeostasis, described by the Ising model, the stochastic resonance (SR) is a counterintuitive phenomenon in which the addition of noise to a nonlinear system improves its detection of weak signals. The critical divergence in how the Ising and spin-glass models process information and energy is the difference between the healthy and malignant tissue processes. At T_{tr} the Ising system is poised at criticality. The correlation length $\xi \to \infty$, and the linear susceptibility χ diverges. The system effectively acts as a macroscopic antenna. Because the energy barriers between states vanish at T_{tr}, the system can amplify a weak signal purely through its own scale-free correlations. In this regime, the role of SR is reduced near ideal criticality but becomes dominant in subcritical, metastable systems such as spin-glass-like tumors, as there is no

threshold barrier that requires noise to cross.

However, in the spin-glass model (representing the tumor), the physics are entirely inverted, and stochastic resonance (SR) becomes the primary mechanism of therapeutic action. The mEHT's $1/f$ modulation and stochastic resonance exploit to preferentially disrupt tumor cell signaling, restore the healthy overall homeostatic $1/f$ noise. The biophysical and mathematical breakdown of why SR is vital for disrupting the spin-glass tumor core needs explanation.

In a spin-glass, the system is frozen far below its critical temperature ($T_{eff} \ll T_{g-tr}$) due to the deeply frustrated couplings (J_{ij}). The free-energy landscape is not smooth; it is ultrametric and highly rugged, characterized by deep, isolated valleys (metastable states) separated by massive energy barriers (ΔE).

If you apply a specific, weak, non-thermal intervention (Eq.(9), like the amplitude modulation in mEHT), let's it $E_{nT}(t) = E_0 \cos(\omega t)$. Because the signal is weak to avoid damaging healthy tissue, its energy is far lower than the barrier height: $E_0 \ll \Delta E$. The weak signal without noise merely causes the tumor's state to undergo tiny, linear oscillations at the bottom of its deep, pathological valley. The tumor absorbs the signal but does not change its state. It remains trapped.

This is when SR becomes an important player. SR occurs in non-linear systems when an optimal amount of noise (stochasticity) is added to a weak periodic signal, allowing the system to cross a threshold it could not cross on its own [73]. In the tumor microenvironment, the escape rate over an energy barrier is governed by the Kramers rate:

$$r_K \propto \exp\left(-\frac{\Delta E \pm E_{nT}(t)}{k_B T}\right) \tag{17}$$

where T here represents the stochastic noise (thermal fluctuations or biological noise) and $E_{nT}(t)$ is the weak, periodic nonthermal therapeutic signal acting as a bias. When the noise level T is optimally tuned, it provides just enough random kinetic "jiggling" to push the system near the top of the barrier ΔE. At that exact moment, the weak, periodic signal $E_{nT}(t)$ provides a directed bias. The tumor's state is "kicked" over the barrier, synchronized with the frequency $\omega = 2\pi f$ of the intervention.

Recall that in a spin-glass, linear susceptibility does not diverge, but non-linear susceptibility (χ_{nL}) diverges massively near T_{g-tr} (with an exponent $\gamma \approx 6.0$). Stochastic resonance is the physical engine that exploits this divergence. The noise allows the system to continuously sample the edges of its local potential well. When it does, it enters the highly non-linear regime of the free-energy landscape. By coupling the weak, specific frequency $E_{nT}(t)$ to the system's own biological noise, SR exponentially amplifies the non-linear response, forcing the rigid network to shatter and transition out of its trapped state.

This biophysical translation mathematically explains the dual-action mechanism of why modulated electro-hyperthermia (mEHT) works. The high-frequency carrier (13.56 MHz) wave slightly elevates the local temperature (T). This is not meant to burn the tissue; it acts as the stochastic noise source, raising

the Kramers rate and jiggling the spin-glass. The low-frequency amplitude modulation ($1/f$ for $E_{nT}(t)$) is the weak periodic signal. It holds specific biological information (targeting altered dielectric properties).

Through SR, the localized noise allows the malignant cells to reach the threshold of their rigid homeostatic valleys, and the weak modulation (signal) pushes them over the edge into apoptosis. The cancerous energy landscape is modeled by spin-glass, diverges by the amplitude of the electromagnetic field signal (Figure 5). The $1/f$ noise sends extreme stochastic pushes. Without the stochastic $1/f$ signal, the noise just causes random, undirected thermal agitation. Together, they break the spin-glass.

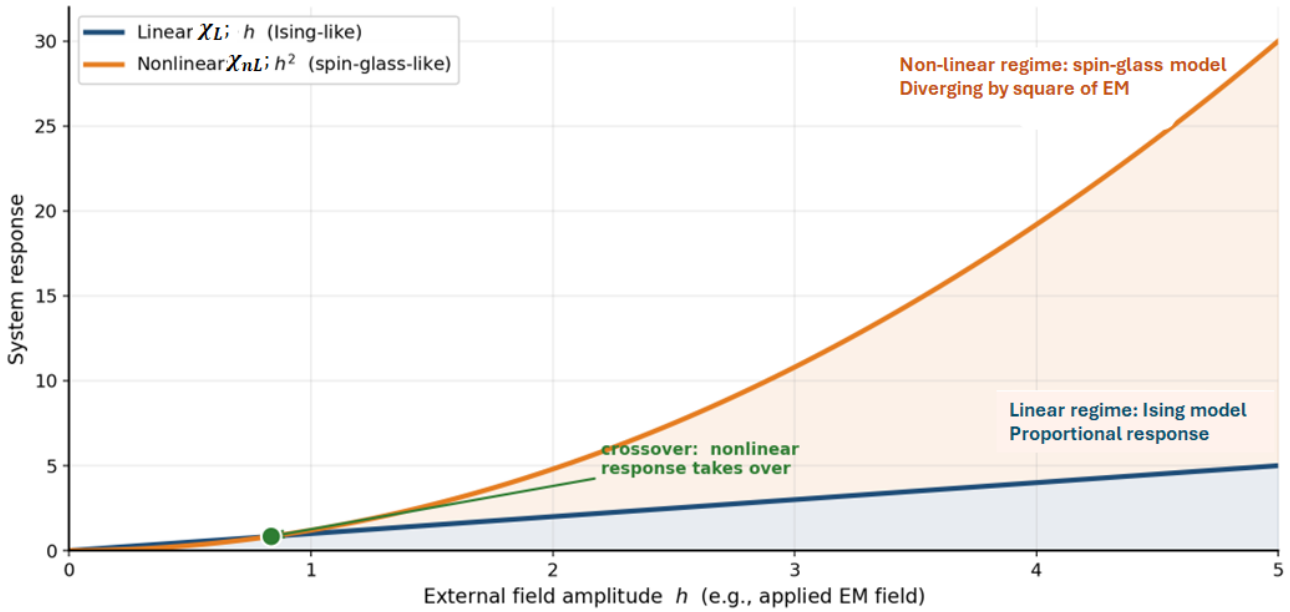

Figure 5. The linearly responding Ising energy minimum is overtaken by the pathology of the nonlinear responder. This larger electromagnetic sensitivity of malignant tissue is one of the selective factors of mEHT, when the stochastic and intensive $1/f$ pushed by extreme amplitudes of the modulation when $f \approx 0$.

5.3. Immunogenic Processes

Beyond membrane effects, the thermal component of mEHT (microscopic local temperature elevation to 40˚C - 43˚C in tumor cells) activates heat shock protein (HSP) expression, HSP70, HSP90, and HSP27, which function as molecular chaperones [74]. Interestingly, the dynamics of protein folding and aggregation under thermal stress can themselves be modeled as Ising-like systems, with the folded/unfolded state of a protein corresponding to spin configurations in a heteropolymer model. Near the folding transition temperature, protein conformational fluctuations are maximal, and the system is most sensitive to external perturbations (such as elevated temperature). mEHT-induced thermal stress thus drives the protein conformational ensemble of tumor cells toward a critical regime of maximal sensitivity, thereby facilitating HSP-dependent immune recognition and activation of the apoptotic pathway [74].

Recent experimental evidence indicates that mEHT induces immunogenic cell death (ICD) in tumor cells [75] [76], characterized by calreticulin surface exposure, HMGB1 release, and ATP secretion, danger signals that activate dendritic cells and prime anti-tumor T-cell responses [77]. The abscopal effect, regression of non-irradiated distant metastases following local mEHT treatment, has been reviewed preclinically [78], and clinically [79] [80] and attributed to this systemic immune activation [81]. From an Ising perspective, ICD can be understood as a coordinated, collective phase transition of the tumor cell population triggered by the disruption of its spin-glass-like phenotypic metastability: the mEHT perturbation drives the tumor from its metastable spin-glass states toward a globally stable apoptotic phase.

5.4. Effect on the Cell Membrane

The cell membrane has special arrangements, including transmembrane proteins, channels, junctions, and adherent connections. In healthy cells, these structures are connected to the well-organized, polymerized cytoskeleton, forming an organic, integrated connection between the cellular machinery and the environment. The membrane is a two-dimensional layer that allows easy lateral movement and has high potential. The structures embedded in the lipid matrix are cytoskeletal-restricted linear corrals, with specific roles in sensing, transport, and defense mechanisms. In cellular division and cancer, the cytoskeletal structure collapses and is rearranged by polymerization to produce the daughter cells. This transition is framed as the shift from cytoskeleton-restricted linear corrals (the "one-dimensional", 1D state) to macro-clustered lipid rafts (the 2D state). In a healthy process, the newly polymerized cytoskeleton re-forms the linear corals, reducing the number of rafts, whereas in cancer, the large number of rafts remains on the surface [82]. This structural shift was observed using super-resolution microscopy (such as STORM and PALM) and Single-Particle Tracking (SPT).

Ion channel mechanisms play a critical role in the cell's fate. Ion channel gating is not an isolated stochastic event but a cooperative phenomenon that can be modeled by an Ising system, explaining how the 1D cytoskeleton-restricted linear corrals collapse on the membrane and the transmembrane proteins form rafts, 2D lipid-rich clusters instead [83]. The model provides a framework in which how a weak, targeted intervention explain could induce cooperative gating, offering a candidate explanation for the observed efficacy and selectivity of mEHT at the membrane level.

5.4.1. The Core Mapping: Gating as a Cooperative Channel State

The state of an ion channel (e.g., a Ca^{2+} channel or TRPV1 receptor) is assigned a spin variable $\sigma_i = \pm 1$ (closed/open). The external field of mEHT ($\boldsymbol{E}_{mEHT}$) is explicitly the amplitude-modulated radiofrequency field of mEHT. The coupling constant (J) represents the mechanical or electrostatic interaction between adjacent channels in the lipid bilayer.

mEHT does not need to have sufficient energy to independently open every ion channel on the membrane. If the channels are cooperatively linked ($J > 0$), mEHT only needs to provide enough targeted energy to flip a critical nucleus of highly susceptible channels. The positive coupling J will then drive an avalanche effect, causing a massive, synchronized gating event (like a catastrophic Ca^{2+} influx) that triggers apoptosis.

Healthy cells and malignant cells possess fundamentally different plasma membrane architectures. Malignant membranes have altered lipid raft densities, higher cholesterol content, distinct receptor clustering, and are mechanically more rigid [84]. Consequently, the coupling constant in healthy tissue (J_H) is entirely different from the coupling constant in tumor tissue (J_T). The malignant receptor clustering artificially inflates J_T within localized 2D patches (lipid rafts). By inserting a larger J, the malignant channel clusters sit much closer to a critical phase transition than healthy membranes [83]. Therefore, the exact same external mEHT field $\boldsymbol{E}_{mEHT}$ will trigger a cooperative avalanche in the malignant cell, while acting as harmless, sub-threshold noise in the healthy cell. The dimensionality is crucial for the phase transition. The 1D Ising model do not have a finite-temperature phase transition, while the 2D model exhibits true phase transitions at a finite critical temperature (T_c). If healthy ion channels are distributed sparsely or linearly along cytoskeletal tethers (acting like a 1D system), they resist sudden macroscopic state changes.

Despite the low mechanical shear and liquid-like horizontal mobility, a healthy plasma membrane is not a free-flowing 2D liquid-state. It is tightly regulated by an underlying structural meshwork of the cortical actin cytoskeleton. Using high-speed SPT technology, it was observed that ion channels and receptors do not diffuse randomly in two dimensions; instead, they exhibit compartmentalized diffusion ("hop diffusion") [85]. While the fluid-mosaic model [86] suggested a homogeneous 2D liquid where molecules move via simple Brownian motion, it has been proven that the membrane is highly structured [85]. The channels are physically tethered to or trapped within linear barriers created by actin filaments [87]. They can only slide back and forth along these 1D cytoskeletal tracks, occasionally hopping to an adjacent track. Because they are strung out linearly, their coupling constant (J) with one another is extremely low. They operate largely independently, preventing accidental, massive cooperative gating (which would trigger unwanted apoptosis or depolarization) [87].

When a cell undergoes malignant transformation (such as the Epithelial-Mesenchymal Transition, EMT), it must dismantle its rigid actin cytoskeleton to become motile and invasive [88]. Simultaneously, cancer cells drastically upregulate cholesterol and sphingolipid synthesis. The linear actin steric barrier breaks down, and the membrane channels are suddenly free to diffuse in two dimensions, as was observed with super-resolution microscopy (STORM/STED) [89]. Driven by the high cholesterol content, these channels undergo spontaneous phase separation, aggregating into dense, 2D micro-domains, lipid rafts. So

the consequence of cytoskeletal collapse is lipid raft aggregation, forming new 2D structures on the membrane. The channels are no longer isolated on 1D tracks. They are packed side-by-side in a 2D lattice. This massive spatial proximity radically increases their coupling constant (J). The channels now function as a single, cooperative thermodynamic unit [83].

The 1D→2D transition has been specifically observed in several key ion channels implicated in cancer progression. In healthy adult tissue, the voltage-gated sodium channel 1.5 (Nav1.5) is primarily restricted to highly organized, linear striated domains (like the T-tubules of cardiac muscle). However, in highly metastatic breast cancer (such as MDA-MB-231 cells), Nav1.5 is highly overexpressed and completely alters its spatial distribution [90] [91]. Confocal and super-resolution imaging reveal that these channels cluster densely into 2D lipid rafts. Transient Receptor Potential (TRP) channels, which regulate calcium (Ca^{2+}) influx, are deeply tied to apoptosis. In healthy cells, they are distributed sparsely [92]. In prostate and breast cancers, lipidomics and fluorescence microscopy confirm that TRP channels aggregate into massive, dense 2D raft clusters to amplify pro-survival signaling [93].

The direct observation of this cytoskeletal-to-raft transition selectively offers a candidate mechanistic account of the observed selectivity of mEHT, involving the voltage-sensitive [94] and TRP [95] channels. By forcing the tumor's ion channels into dense 2D clusters to aid in its own invasive signaling, the cancer cell inadvertently builds a macroscopic, highly cooperative sensing system. The disruption of the lipid raft matrix, as the mEHT nonthermal effect does with resonances, ceases the cooperative gating of the TRPV1 channels [96].

The healthy channels (still isolated on their 1D actin tracks) cannot cooperate sufficiently to cross the gating threshold, under the nonthermal force of the mEHT field ($\boldsymbol{E}_{mEHT}$). But the tumor's clustered channels, bound by high 2D coupling (J), absorb the amplitude-modulated frequency cooperatively. They experience a massive, synchronized gating avalanche that floods the malignant cell with lethal levels of Ca^{2+} and together with numerous other factors, triggers apoptosis [97].

When malignant transformation causes transmembrane proteins and channels to aggregate into dense 2D lipid rafts, the system shifts mathematically into the 2D Ising universality class. This shift gives the tumor an ordered, rigid membrane microdomain, but paradoxically introduces a T_c. mEHT specifically exploits this newly acquired 2D criticality, thereby forcing the rafts to absorb energy through targeted resonance.

5.4.2. Dynamic Equilibrium with $1/f$ Noise

The dynamic equilibrium forced by the $1/f$ noise allows to extend the static Ising model into a dynamic Ising arrangement [98] [99]. The cooperative gating of ion channels under healthy biological conditions produces $1/f$ noise. A dynamic framework has to be studied with a stochastic kinetic model to explain the dynamic equilibrium of $1/f$ noise with mEHT application.

Two distinct types of movement occur in biological membranes, which could be modeled by dynamical Ising models: channel gating (opening/closing) [98], and physical diffusion of channels across the lipid bilayer (clustering into rafts) [99].

The gating dynamics simulate systems where the order parameter (the total number of open channels) is not conserved [98]. A channel can spontaneously flip its state $\sigma_i \to -\sigma_i$, $\sigma_i \in \{-1,1\}$ (closed ↔ open) based on interactions with its neighbors and the external environment. To model the mEHT intervention, we introduce a time-varying external electric field $\boldsymbol{E}_{mEHT} = \boldsymbol{E}_0 \cos(\omega t)$ into the local Hamiltonian.

The probability $P(\sigma_1, \cdots, \sigma_N, t)$ of finding the membrane in a specific configuration evolves according to the Master Equation. The transition rate $W(\sigma_i \to -\sigma_i)$ for a single channel to flip is governed by the energy change ΔE_i:

$$\Delta E_i = 2\sigma_i \left(J \sum_{\langle j \rangle} \sigma_j + \mu \boldsymbol{E}_0 \cos(\omega t) \right) \tag{18}$$

and the transition probability:

$$W(\sigma_i \to -\sigma_i) = \frac{1}{2\tau_0} \left[1 - \sigma_i \tanh\left(\frac{\beta \Delta E_i}{2} \right) \right] \tag{19}$$

where τ_0 is the intrinsic gating time of an isolated channel, and $\beta = \frac{1}{k_B T}$.

This formulation is critical for defining the dynamic susceptibility $\chi(\omega)$ of the membrane. Because malignant cells feature clustered, highly cooperative channels (large J), their effective relaxation time (τ) slows down dramatically compared to healthy cells, leading to a critical slowing phenomenon.

$$\tau_{malignant} \gg \tau_{healthy} \tag{20}$$

When the mEHT frequency ω is tuned to match the inverse of this sluggish malignant relaxation time ($\omega \approx 1/\tau_{malignant}$), the oscillating field locks onto the gating mechanism. The malignant channels undergo massive, resonant power absorption, forcing them into a synchronized, continuous open state. The healthy channels, possessing a much faster $\tau_{healthy}$, merely experience the mEHT field as a negligible, sub-threshold high-frequency blur.

The spatial arrangement is also described by the dynamic Ising model [99]. In this model the order parameter (the total number of channels) is conserved, but adjacent σ_i positions (representing a channel and an empty lipid space) can exchange locations. This is the physics of lateral membrane diffusion and the formation of the 2D lipid rafts.

A channel at position i swaps with a lipid molecule at position k. The transition rate depends on the energy difference of the entire macroscopic state before and after the swap:

$$W(\sigma_i \to -\sigma_i) = \frac{1}{\tau_D} \frac{\exp(-\beta \Delta E_{ik})}{1 + \exp(-\beta \Delta E_{ik})} \tag{21}$$

where τ_D is the characteristic lateral diffusion time.

Healthy homeostatic regulation requires fluidity; channels must be able to diffuse, aggregate transiently, and disperse. This produces the characteristic healthy $1/f$ noise spectrum in membrane capacitance and signaling. In the malignant state, altered cholesterol levels push the local interaction J so high that the exchange rate plummets. The channels become spatially locked into rigid, semi-permanent rafts.

By applying an external oscillating field $\boldsymbol{E}_{mEHT}(t)$ at the exact frequency of the modulation in audio (α-dispersion) range (100 Hz - 5 kHz), the phase lag of the channel gating can be calculated. In these conditions, mEHT drives the stochastic process. The mEHT field $\boldsymbol{E}_{mEHT}(t)$, results in resonant energy absorption that locally raises the effective thermal noise (T) within the raft domain. This localized heating lowers the β parameter precisely at the raft boundary, suddenly accelerating the exchange rate and literally "melting" the clustered receptors back into the fluid lipid phase, severing the tumor's dysregulated signaling cascade.

A complete framework is established for how healthy $1/f$ noise is generated and subsequently destroyed in pathology by combining the two dynamics, the channel gating (opening/closing) [98], and physical diffusion of channels across the lipid bilayer (clustering into rafts) [99]. In a healthy state (low J), the gating and diffusion are balanced. The system fluctuates continuously across multiple scales of time and space, generating a scale-free $1/f$ power spectrum. However, in a malignant state (high J) the strong coupling suppresses diffusion (trapping channels in rafts) and slows gating. The noise spectrum shifts away from $1/f$ toward restricted, low-frequency oscillations (glassy dynamics).

The mEHT Intervention with the targeted time-varying field $\boldsymbol{E}_{mEHT}(t)$ forces the gating in the malignant, high-J regions to rapidly flip at the frequency ω. This forced oscillation shatters the spatial domains, dissolving the malignant correlation.

5.5. Therapeutic Implications of $1/f$ Noise—mEHT Interventions in the Ising Frame

If $1/f$ noise is a signature of criticality, and if criticality is the healthy operating point, then therapeutic strategies that restore $1/f$ noise structure may be intrinsically health-promoting. This principle has been explored in several contexts [100]. Stochastic resonance-based therapies, in which sub-threshold noise is added to sensory or motor pathways to improve signal detection and motor control, have shown efficacy in Parkinson's disease, diabetic neuropathy, and balance disorders in the elderly. The application of $1/f$-distributed mechanical vibration to bone and muscle has been proposed as a countermeasure against the loss of musculoskeletal complexity with aging.

1) The therapeutic implications of the power of $1/f$ in mEHT is the modulation. Properly chosen noise can transfer free energy to support cellular reactions

[101]. The dynamic relations produce a noise of homeostatic equilibrium, which is measured as a peculiar signal [4] [45]. This noise differs between malignant and healthy tissue and is measurable as the RF current [102]. At the critical point (T_c) of an Ising system, the power spectral density of fluctuations naturally follows a $1/f$ (pink noise) pattern. This suggests that the bioelectromagnetic $1/f$ noise is the natural communication language of a system [103], and the Ising model is a proxy for multicellularity.

2) Malignant cells are often stuck in a disordered, non-critical regime. By applying external $1/f$ fluctuations, mEHT acts as a catalyst, pushing the cellular network back toward its critical point. It lowers the energy barrier required for the system to undergo a phase transition, in this case, transitioning from a state of uncontrolled growth to programmed death.

3) In the Ising frame, the interacting particles (Ising spins) can be represented by signaling proteins in membrane rafts. The $1/f$ spectrum matches the natural dwell times of these protein aggregates, selectively excites the membrane rafts of malignant cells. This enables stochastic resonance, in which noise energy selectively amplifies the signaling of apoptotic pathways (such as FAS/TRAIL) without requiring excessive heat, thus preserving healthy tissue.

4) Because the Ising frame emphasizes neighbor-to-neighbor interactions, the therapy does not just kill individual cells; it triggers a phase transition in the microenvironment. This promotes induction of collective apoptosis, immunogenic cell death (ICD). The $1/f$ signal helps synchronize the release of damage-associated molecular patterns (DAMPs), effectively "re-coupling" the tumor cells to the body's immune system, turning a local treatment into a systemic (abscopal) response.

Based on the current trajectory of biophysics and mEHT research, the future lies in "Informational Oncology" (Table 3).

Table 3. The innovation area of "informational oncology".

Innovation Area	Description
Adaptive α Modulation	Real-time tuning of the modulation exponent (α) based on the patient's individual homeostatic signature to maximize resonance.
Phase-Transition Mapping	Using the Ising frame to predict which tumors are most "brittle" (not in but close to criticality) and therefore most susceptible to low-energy $1/f$ interventions, which re-establishes the criticality, the normal living at the edge of chaos.
Synthetic Homeostasis	Combining $1/f$ mEHT with immunotherapy to force malignant clusters to adopt a multicellular "social" behavior before inducing targeted apoptosis.

6. Synthesis: A Unified Biophysical Framework

The threads converge on a coherent, testable biophysical framework. Healthy multicellular organisms maintain their component subsystems, from individual cell membranes to organ-level physiological networks, near the critical point of effective Ising-like phase transitions. This criticality is not a coincidence but an

evolved property, maintained by homeostatic feedback loops, that enables maximal adaptive capacity. Disease, and cancer in particular, represents a departure from criticality. The specific direction of departure, toward excess order or excess disorder, varies by disease type and stage, but the unifying feature is the loss of scale-free, $1/f$ dynamics and the reduction of functional complexity.

The $1/f$ noise is the signature of criticality in living systems. Its measurement provides a non-invasive, quantitative index of physiological health status, a complex biomarker that integrates the collective behavior of thousands of coupled elements into a single, interpretable number. mEHT exerts its anti-tumor effects through multiple, mechanistically interconnected pathways, membrane domain interactions, proteotoxic stress, and immunogenic cell death, all of which can be understood as perturbations of a spin-glass-like tumor system away from its metastable states. The $1/f$ modulation of mEHT is designed to resonate with the natural dynamics of critical biological systems, providing selectivity between healthy (critical) and tumor (off-critical) tissue.

The Ising model and its generalizations (spin glasses, random-field Ising models, quantum Ising models) provide the mathematical language to formalize these ideas, generate testable quantitative predictions, and guide the rational design of therapeutic interventions targeting the critical properties of biological matter.

7. Outstanding Challenges and Future Directions

Despite the conceptual elegance and growing empirical support for the criticality hypothesis, several important challenges remain. The Ising model description has different drawbacks in describing the living cellular interactions:

- Healthy tissue thrives on functional differentiation. A healthy lattice is not a collection of identical "up" states; it is a highly choreographed arrangement of diverse cell types (parenchymal, stromal, immune) with varying coupling constants J_{ij}. Treating healthy tissue as a uniform Ising lattice ignores the spatial non-uniformity that is actually a hallmark of health and resilience.
- Healthy biological states are rarely binary. Cells exist in a continuum of metabolic activities, differentiation stages, and signaling states. Health is characterized by multistability, the ability to switch between many functional modes. Reducing this to "Alive/Dead" or "Cooperative/Autonomous" misses the nuanced regulatory "gray zones" that allow for homeostatic adjustment.
- The interactions between the cells are not constant in the healthy interactions, as the Ising model uses, and not distributed by a Gaussian, as the spin-glass model predicts. These approximations are valid on average.
- Bioelectrodynamics and endocrine signaling are long-range. A cell in one part of an organ can influence another far away via bioelectric fields or systemic signals. The living tissue has longer interactions with the nearest neighbors (e.g., messenger molecules, electrodiffusion, etc.), but the neighbors still have the largest.

- Healthy life is a dissipative structure operating far from equilibrium. It doesn't want to "settle" into a ground state; it wants to maintain a flow of energy and matter. The temporal dynamics of energy flux are absent.
- Living tissue is dynamic. Cells migrate, the extracellular matrix remodels, and the "topology" of the interaction changes in real-time. In a healthy object, the "spins" move. A model with fixed coordinates cannot easily account for the structural plasticity of healthy development and wound healing.
- The strong coupling constant in the Ising model makes the system "brittle," increasing the T_c and shifting the system away from the "edge of chaos" living fluctuations. However, the strong junctions and adherent connections do not weaken; on the contrary, they improve healthy homeostatic control. These interactions are neglected in the Ising model, which focuses only on field interactions. This drawback is not critical for the mEHT application, which operates only in fields.

Despite these drawbacks, the Ising model well describes the main dynamic changes in the "edge of chaos" homeostasis, and the spin-glass model well corresponds to the main features of malignancy that deviate from the critical "edge" dynamic status.

- Distinguishing criticality from near-criticality. Power-law statistics consistent with criticality can arise from non-critical systems through superposition of log-normally distributed relaxation times (the Lorentzian superposition model), making rigorous discrimination between true SOC and mere scale-free statistics non-trivial. Finite-size scaling analyses, higher-order statistics, and the collapse of data from systems of different sizes onto universal scaling functions are necessary to establish genuine criticality.
- The role of quantum effects. Biological systems are warm, wet, and noisy, conditions historically considered hostile to quantum coherence. Nevertheless, evidence for quantum effects in photosynthetic energy transfer, avian magnetoreception, and olfaction has challenged this assumption. At the membrane level, the question of whether quantum fluctuations play a role in proximity to the lipid miscibility critical point, and whether quantum Ising dynamics are relevant to biological criticality, remains open and theoretically rich.
- From correlation to causation in disease. The observation that cancer cells and diseased tissues show altered $1/f$ dynamics is established, but the causal direction requires clarification: does loss of criticality cause pathology, or does pathology cause loss of criticality? Longitudinal studies tracking complexity biomarkers before and during disease onset, combined with experimental models in which criticality is artificially tuned, are needed to resolve this question.
- Further clinical translation of mEHT biophysics and technique. Research on mechanistic biomarkers, including HRV-derived complexity indices [41], membrane lipid raft biomarkers, and tumor microenvironment imaging, is

needed to further improve the technique and optimize treatment parameters. In addition to the compelling biophysical rationale for mEHT and the wide range of preclinical studies [78], and numerous real-world ITT clinical studies [79] [104] [105], as well as some rigorous Phase II. studies [106], and one Phase III randomized controlled trial with biomarker-stratified patient populations [107], further clinical studies are necessary for wider acceptance of mEHT in oncology.

8. Conclusions

The Ising model holds an extraordinary position in the intellectual landscape of modern biophysics: it is simultaneously a simple mathematical abstraction, a rigorous statistical-mechanical theory, and a flexible metaphorical framework that illuminates deep connections among phase transitions, criticality, and the organization of living matter. Nevertheless, do not forget that it is a model, not the complex reality; however, it can describe a part of the living characteristics: the edge of chaos, as the intrinsic behavior of living systems. From the scale-free fluctuations of neural networks to the lipid raft dynamics of the cancer cell membrane, from the $1/f$ noise of the healthy heartbeat to the spin-glass metastability of the tumor microenvironment, Ising physics provides a unifying thread.

We have argued that life, at multiple scales, operates at the edge of a phase transition, and that this positioning is not accidental but functional: criticality confers maximal sensitivity, adaptability, and information processing capacity. Health is the maintenance of this critical edge; disease is its disruption. The $1/f$ power spectrum is the observable signature of criticality, providing both a diagnostic window into the state of a biological system and a therapeutic target for interventions designed to restore critical dynamics.

Modulated electro-hyperthermia represents one of the most sophisticated current attempts to exploit this biophysical understanding therapeutically, delivering electromagnetic energy with a spectral structure matched to the natural dynamics of critical biological systems, selectively targeting the off-critical, spin-glass-like tumor tissue while sparing the healthy, critical-regime normal tissue. As the biophysical foundations of mEHT are further elucidated, and as the connections between criticality and cancer biology deepen, we anticipate that the Ising model will continue to serve as an indispensable conceptual tool for the translation of fundamental physics into clinical benefit.

Conflicts of Interest

The author declares no conflicts of interest regarding the publication of this paper.

References

[1] Kurakin, A. (2011) The Self-Organizing Fractal Theory as a Universal Discovery Method: The Phenomenon of Life. *Theoretical Biology and Medical Modelling*, **8**,

Article No. 4. https://doi.org/10.1186/1742-4682-8-4

[2] Walleczek, J. (2000) Self-Organized Biological Dynamics & Nonlinear Control. Cambridge University Press.

[3] Sornette, D. (2000) Chaos, Fractals, Self-Organization and Disorder: Concepts and Tools. Springer Verlag.

[4] West, B.J. (1990) Fractal Physiology and Chaos in Medicine. World Scientific. https://doi.org/10.1142/1025

[5] Kauffman, S.A. (1993) The Origins of Order: Self-Organization and Selection in Evolution. Oxford University Press.

[6] Brummer, A.B., Savage, V.M. and Enquist, B.J. (2017) A General Model for Metabolic Scaling in Self-Similar Asymmetric Networks. *PLOS Computational Biology*, **13**, e1005394. https://doi.org/10.1371/journal.pcbi.1005394

[7] Ochiai, T., Nacher, J.C. and Akutsu, T. (2018) Symmetry and Dynamics in Living Organisms: The Self-Similarity Principle Governs Gene Expression Dynamics. https://arxiv.org/abs/q-bio/0503003

[8] Bassingthwaighte, J.B., Leibovitch, L.S. and West, B.J. (1994) Fractal Physiology. Oxford University Press.

[9] Glazier, D.S. (2014) Metabolic Scaling in Complex Living Systems. *Systems*, **2**, 451-540. https://doi.org/10.3390/systems2040451

[10] West, G.B., Woodruff, W.H. and Brown, J.H. (2002) Allometric Scaling of Metabolic Rate from Molecules and Mitochondria to Cells and Mammals. *Proceedings of the National Academy of Sciences*, **99**, 2473-2478. https://doi.org/10.1073/pnas.012579799

[11] Li, W. (1989) Spatial 1/*f* Spectra in Open Dynamical Systems. *Europhysics Letters* (*EPL*), **10**, 395-400. https://doi.org/10.1209/0295-5075/10/5/001

[12] Shlesinger, M.F. (1987) Fractal Time and 1/f Noise in Complex Systems. *Annals of the New York Academy of Sciences*, **504**, 214-228. https://doi.org/10.1111/j.1749-6632.1987.tb48734.x

[13] West, G.B. and Brown, J.H. (2005) The Origin of Allometric Scaling Laws in Biology from Genomes to Ecosystems: Towards a Quantitative Unifying Theory of Biological Structure and Organization. *Journal of Experimental Biology*, **208**, 1575-1592. https://doi.org/10.1242/jeb.01589

[14] Aon, M.A., Saks, V. and Schlattner, U. (2014) Systems Biology of Metabolic and Signaling Networks: Energy, Mass and Information Transfer. Springer Series in Biophysics No. 16. Springer.

[15] Fröhlich, H. (1983) Coherence in Biology. In: Frohlich, H. and Kremer, F., Eds., *Coherent Excitations in Biological Systems*, Springer, 1-5. https://doi.org/10.1007/978-3-642-69186-7_1

[16] Frohlich, H. (1988) Biological Coherence and Response to External Stimuli. Springer Verlag.

[17] Goff, L.L. and Lecuit, T. (2009) Phase Transition in a Cell. *Science*, **324**, 1654-1655. https://doi.org/10.1126/science.1176523

[18] Milazzo, G. (1988) Applications of Bioelectrochemistry in Medicine. *Bioelectrochemistry and Bioenergetics*, **19**, 191-205. https://doi.org/10.1016/0302-4598(88)80001-1

[19] Adey, W.R. (1993) Biological Effects of Electromagnetic Fields. *Journal of Cellular Biochemistry*, **51**, 410-416. https://doi.org/10.1002/jcb.2400510405

[20] Sowers, A.E. (1984) Characterization of Electric Field-Induced Fusion in Erythrocyte Ghost Membranes. *The Journal of Cell Biology*, **99**, 1989-1996. https://doi.org/10.1083/jcb.99.6.1989

[21] Marszalek, P. and Tsong, T.Y. (1995) Cell Fission and Formation of Mini Cell Bodies by High Frequency Alternating Electric Field. *Biophysical Journal*, **68**, 1218-1221. https://doi.org/10.1016/s0006-3495(95)80338-3

[22] Mun, E.J., Babiker, H.M., Weinberg, U., Kirson, E.D. and Von Hoff, D.D. (2018) Tumor-Treating Fields: A Fourth Modality in Cancer Treatment. *Clinical Cancer Research*, **24**, 266-275. https://doi.org/10.1158/1078-0432.ccr-17-1117

[23] Grondin, Y., Raine, D.J. and Norris, V. (2012) Life at the "Edge of Chaos" in a Genetic Model. In: Minai, A.A., Braha, D. and Bar-Yam, Y., Eds., *Unifying Themes in Complex Systems VII*, Springer, 124-131. https://doi.org/10.1007/978-3-642-18003-3_12

[24] Hanel, R., Pöchacker, M. and Thurner, S. (2010) Living on the Edge of Chaos: Minimally Nonlinear Models of Genetic Regulatory Dynamics. *Philosophical Transactions of the Royal Society A*: *Mathematical*, *Physical and Engineering Sciences*, **368**, 5583-5596. https://doi.org/10.1098/rsta.2010.0267

[25] Lewin, R. (1992) Complexity, Life at the Edge of Chaos. University of Chicago Press.

[26] Ising, E. (1925) Beitrag zur Theorie des Ferromagnetismus. *Zeitschrift für Physik*, **31**, 253-258. https://doi.org/10.1007/bf02980577

[27] Onsager, L. (1944) Crystal Statistics. I. A Two-Dimensional Model with an Order-Disorder Transition. *Physical Review*, **65**, 117-149. https://doi.org/10.1103/physrev.65.117

[28] Szász, A. (1985) One Possible Analytical Approximation of the Critical Point of the Three-Dimensional Ising Model. *Physica Status Solidi* (*B*), **130**, K97-K100. https://doi.org/10.1002/pssb.2221300250

[29] Szasz, A. (2026) Approximate Algebraic Solution of 3D Ising Model—Transfer-Matrix Method. *Advances in Pure Mathematics*, **16**, 395-411. https://doi.org/10.4236/apm.2026.166021

[30] Langton, C.G. (1990) Computation at the Edge of Chaos: Phase Transitions and Emergent Computation. *Physica D*: *Nonlinear Phenomena*, **42**, 12-37. https://doi.org/10.1016/0167-2789(90)90064-v

[31] Beggs, J.M. and Plenz, D. (2003) Neuronal Avalanches in Neocortical Circuits. *The Journal of Neuroscience*, **23**, 11167-11177. https://doi.org/10.1523/jneurosci.23-35-11167.2003

[32] Tkačik, G., Mora, T., Marre, O., Amodei, D., Palmer, S.E., Berry, M.J., *et al.* (2015) Thermodynamics and Signatures of Criticality in a Network of Neurons. *Proceedings of the National Academy of Sciences*, **112**, 11508-11513. https://doi.org/10.1073/pnas.1514188112

[33] Janke, W. (1996) Monte Carlo Simulations of Spin Systems. In: Hoffmann, K.H. and Schreiber, M., Eds., *Computational Physics*, Springer, 10-43. https://doi.org/10.1007/978-3-642-85238-1_3

[34] Fröhlich, H. (1982) What Are Non-Thermal Electric Biological Effects? *Bioelectromagnetics*, **3**, 45-46. https://doi.org/10.1002/bem.2250030109

[35] Schwan, H.P. (1982) Nonthermal Cellular Effects of Electromagnetic Fields: AC-Field Induced Ponderomotoric Forces. *British Journal of Cancer*, **45**, 220-224.

[36] Fortel, I., Butler, M., Korthauer, L.E., Zhan, L., Ajilore, O., Sidiropoulos, A., *et al.* (2022) Inferring Excitation-Inhibition Dynamics Using a Maximum Entropy Model Unifying Brain Structure and Function. *Network Neuroscience*, **6**, 420-444. https://doi.org/10.1162/netn_a_00220

[37] Jain, V., Koehler, F. and Risteski, A. (2019) Mean-Field Approximation, Convex Hierarchies, and the Optimality of Correlation Rounding: A Unified Perspective. *Proceedings of the* 51*st Annual ACM SIGACT Symposium on Theory of Computing*, Phoenix, 23-26 June 2019, 1226-1236. https://doi.org/10.1145/3313276.3316299

[38] Kirkley, A., Cantwell, G.T. and Newman, M.E.J. (2021) Belief Propagation for Networks with Loops. *Science Advances*, **7**, eabf1211. https://doi.org/10.1126/sciadv.abf1211

[39] Ferrenberg, A.M., Xu, J. and Landau, D.P. (2018) Pushing the Limits of Monte Carlo Simulations for the Three-Dimensional Ising Model. *Physical Review E*, **97**, Article ID: 043301. https://doi.org/10.1103/physreve.97.043301

[40] Bak, P., Tang, C. and Wiesenfeld, K. (1988) Self-Organized Criticality. *Physical Review A*, **38**, 364-374. https://doi.org/10.1103/physreva.38.364

[41] Szasz, A. (2022) Stimulation and Control of Homeostasis. *Open Journal of Biophysics*, **12**, 89-131. https://doi.org/10.4236/ojbiphy.2022.122004

[42] Goldberger, A.L., Amaral, L.A.N., Hausdorff, J.M., Ivanov, P.C., Peng, C. and Stanley, H.E. (2002) Fractal Dynamics in Physiology: Alterations with Disease and Aging. *Proceedings of the National Academy of Sciences*, **99**, 2466-2472. https://doi.org/10.1073/pnas.012579499

[43] Lipsitz, L.A. and Goldberger, A.L. (1992) Loss of "Complexity" and Aging. *JAMA*, **267**, 1806-1809. https://doi.org/10.1001/jama.1992.03480130122036

[44] Szasz, O., Szasz, M.A., Minnaar, C. and Szasz, A. (2017) Heating Preciosity—Trends in Modern Oncological Hyperthermia. *Open Journal of Biophysics*, **7**, 116-144. https://doi.org/10.4236/ojbiphy.2017.73010

[45] Musha, T. and Sawada, Y. (1994) Physics of the Living State. IOS Press.

[46] Szendro, P., Vincze, G. and Szasz, A. (2001) Bio-Response to White Noise Excitation. *Electro- and Magnetobiology*, **20**, 215-229. https://doi.org/10.1081/jbc-100104145

[47] Szendro, P., Vincze, G. and Szasz, A. (2001) Pink-Noise Behaviour of Biosystems. *European Biophysics Journal*, **30**, 227-231. https://doi.org/10.1007/s002490100143

[48] Ito, K. and Gunji, Y. (1994) Self-Organisation of Living Systems Towards Criticality at the Edge of Chaos. *Biosystems*, **33**, 17-24. https://doi.org/10.1016/0303-2647(94)90057-4

[49] Prigogine, I. and Stengers, I. (1985) Order Out of Chaos. Flamingo.

[50] Olszewska, M., Haduch-Sendecka, A. and Pietruszka, M. (2018) Determination of Selected Dynamic Quantities of Growing Intact Seeds of Maize. *General Physiology and Biophysics*, **37**, 375-389. https://doi.org/10.4149/gpb_2017058

[51] Pietruszka, M. and Olszewska, M. (2020) Extracellular Ionic Fluxes Suggest the Basis for Cellular Life at the 1/f Ridge of Extended Criticality. *European Biophysics Journal*, **49**, 239-252. https://doi.org/10.1007/s00249-020-01430-3

[52] Pruessner, G. (2012). Self-Organised Criticality. Theory, Models and Characterization. Cambridge University Press. https://doi.org/10.1017/cbo9780511977671

[53] Szasz, A. and Szasz, O. (2020) Ch. 17. Time-Fractal Modulation of Modulated Electro-Hyperthermia (mEHT). In: Szasz, A., Ed., *Challenges and Solutions of Oncolog-*

ical Hyperthermia, Cambridge Scholars, 377-415.

[54] Szasz, A. (2022) Time-Fractal Modulation—Possible Modulation Effects in Human Therapy. *Open Journal of Biophysics*, **12**, 38-87. https://doi.org/10.4236/ojbiphy.2022.121003

[55] Holmes, F.L. (1986) Claude Bernard, the "Milieu Intérieur", and Regulatory Physiology. *History and Philosophy of the Life Sciences*, **8**, 3-25. http://www.jstor.org/stable/23328847

[56] Brown, T.M. and Fee, E. (2002) Walter Bradford Cannon: Pioneer Physiologist of Human Emotions. *American Journal of Public Health*, **92**, 1594-1595. https://doi.org/10.2105/ajph.92.10.1594

[57] Veatch, S.L. and Keller, S.L. (2005) Seeing Spots: Complex Phase Behavior in Simple Membranes. *Biochimica et Biophysica Acta* (*BBA*)—*Molecular Cell Research*, **1746**, 172-185. https://doi.org/10.1016/j.bbamcr.2005.06.010

[58] Edwards, S.F. and Anderson, P.W. (1975) Theory of Spin Glasses. *Journal of Physics F*: *Metal Physics*, **5**, 965-974. https://doi.org/10.1088/0305-4608/5/5/017

[59] Szigeti, Gy.P., Szasz, A.M. and Szasz, O. (2020) Oncothermia Is a Kind of Oncological Hyperthermia—A Review. *Oncothermia Journal Special Edition*, 2020 September, 8-48. https://www.oncotherm.com/sites/oncotherm/files/2020-09/specialedition01.pdf

[60] Muftuler, T.L., Hamamura, M.J., Birgul, O., *et al.* (2006) *In Vivo* MRI Electrical Impedance Tomography (MREIT) of Tumors. *Technology in Cancer Research, and Treatment*, **5**, 381-387.

[61] Muftuler, L.T., Hamamura, M., Birgul, O. and Nalcioglu, O. (2004) Resolution and Contrast in Magnetic Resonance Electrical Impedance Tomography (MREIT) and Its Application to Cancer Imaging. *Technology in Cancer Research & Treatment*, **3**, 599-609. https://doi.org/10.1177/153303460400300610

[62] Schwan, H.P. (1957) Electrical Properties of Tissue and Cell Suspensions. In: Lawrence, J.H. and Tobias, C.A., Eds., *Advances in Biological and Medical Physics*, Vol. 5, Elsevier, 147-209. https://doi.org/10.1016/b978-1-4832-3111-2.50008-0

[63] Caduff, A., Talary, M.S. and Zakharov, P. (2010) Cutaneous Blood Perfusion as a Perturbing Factor for Noninvasive Glucose Monitoring. *Diabetes Technology & Therapeutics*, **12**, 1-9. https://doi.org/10.1089/dia.2009.0095

[64] Martinsen, O.G., Grimnes, S. and Schwan, H.P. (2002) Interface Phenomena and Dielectric Properties of Biological Tissue. In: Hubbard, A.T., Ed., *Encyclopedia of Surface and Colloid Science*, Marcel Dekker, 2643-2653.

[65] Pething, R. (1979) Dielectric and Electronic Properties of Biological Materials. John Wiley and Sons.

[66] Szasz, O., Andocs, G., Kondo, T., Rehman, M.U., Papp, E., Vancsik, T., *et al.* (2015) Heating of Membrane Rafts of Cancer-Cells. *Journal of Clinical Oncology*, **33**, e22176. https://doi.org/10.1200/jco.2015.33.15_suppl.e22176

[67] Fessler, M.B. and Parks, J.S. (2011) Intracellular Lipid Flux and Membrane Microdomains as Organizing Principles in Inflammatory Cell Signaling. *The Journal of Immunology*, **187**, 1529-1535. https://doi.org/10.4049/jimmunol.1100253

[68] Sviridov, D., Mukhamedova, N. and Miller, Y.I. (2020) Lipid Rafts as a Therapeutic Target. *Journal of Lipid Research*, **61**, 687-695. https://doi.org/10.1194/jlr.tr120000658

[69] Mitra, E.D., Whitehead, S.C., Holowka, D., Baird, B. and Sethna, J.P. (2018) Com-

putation of a Theoretical Membrane Phase Diagram and the Role of Phase in Lipid-Raft-Mediated Protein Organization. *The Journal of Physical Chemistry B*, **122**, 3500-3513. https://doi.org/10.1021/acs.jpcb.7b10695

[70] Sadeghi, S., Müller, M. and Vink, R.L.C. (2014) Raft Formation in Lipid Bilayers Coupled to Curvature. *Biophysical Journal*, **107**, 1591-1600. https://doi.org/10.1016/j.bpj.2014.07.072

[71] Lee, I.-H., Imanaka, M.Y., Modahl, E.H. and Torres-Ocampo, A.P. (2019) Lipid Raft Phase Modulation by Membrane-Anchored Proteins with Inherent Phase Separation Properties. *ACS Omega*, **4**, 6551-6559. https://doi.org/10.1021/acsomega.9b00327

[72] Papp, E., Vancsik, T., Kiss, E. and Szasz, O. (2017) Energy Absorption by the Membrane Rafts in the Modulated Electro-Hyperthermia (mEHT). *Open Journal of Biophysics*, **7**, 216-229. https://doi.org/10.4236/ojbiphy.2017.74016

[73] Szasz, A. (2021) Therapeutic Basis of Electromagnetic Resonances and Signal-modulation. *Open Journal of Biophysics*, **11**, 314-350. https://doi.org/10.4236/ojbiphy.2021.113011

[74] Minnaar, C.A. and Szasz, A. (2022) Forcing the Antitumor Effects of HSPs Using a Modulated Electric Field. *Cells*, **11**, Article No. 1838. https://doi.org/10.3390/cells11111838

[75] Lee, S.Y. and Szasz, A. (2022) Immunogenic Effect of Modulated Electro-Hyperthermia (mEHT) in Solid Tumors. In: Rezaei, N., Ed., *Challenges in Solid Tumors and Other Cancers: An Interdisciplinary Approach*, Springer Nature Switzerland, 185-212. https://doi.org/10.1007/16833_2022_74

[76] Szasz, A. and Szasz, A. (2020) Towards the Immunogenic Hyperthermic Action: Modulated Electrohyperthermia. *Clinical Oncology and Research*, **3**, 1-6. https://doi.org/10.31487/j.cor.2020.09.07

[77] Szasz, A. (2019) Immune-Effects with Local Hyperthermia. *Oncothermia Journal*, **26**, 139-148. https://oncotherm.com/sites/oncotherm/files/2019-07/Immune_effects_with_local_hyperthermia.pdf

[78] Krenacs, T., Meggyeshazi, N., Forika, G., Kiss, E., Hamar, P., Szekely, T., *et al.* (2020) Modulated Electro-Hyperthermia-Induced Tumor Damage Mechanisms Revealed in Cancer Models. *International Journal of Molecular Sciences*, **21**, Article No. 6270. https://doi.org/10.3390/ijms21176270

[79] Szasz, A.M., Minnaar, C.A., Szentmártoni, G., Szigeti, G.P. and Dank, M. (2019) Review of the Clinical Evidences of Modulated Electro-Hyperthermia (mEHT) Method: An Update for the Practicing Oncologist. *Frontiers in Oncology*, **9**, Article No. 1012. https://doi.org/10.3389/fonc.2019.01012

[80] Lee, S.-Y., Lorant, G., Grand, L. and Szasz, A.M. (2023) The Clinical Validation of Modulated Electro-Hyperthermia (mEHT). *Cancers*, **15**, Article No. 4569. https://doi.org/10.3390/cancers15184569

[81] Szasz, O. (2020) Ch. 11. Local Treatment with Systemic Effect: Abscopal Outcome. In: Szasz A., Ed., *Challenges and Solutions of Oncological Hyperthermia*, Cambridge Scholars, 192-205.

[82] Staunton, J.R. and Wirtz, D. (2013) Physical Sciences-Oncology Centers Network. A Physical Sciences Network Charactrization of Non-Tumorigenic and Metastatic Cells. *Scientific Reports*, **3**, Article No. 1449.

[83] Liu, Y. and Dilger, J.P. (1993) Application of the One- and Two-Dimensional Ising

Models to Studies of Cooperativity between Ion Channels. *Biophysical Journal*, **64**, 26-35. https://doi.org/10.1016/s0006-3495(93)81337-7

[84] Galeotti, T., Borrello, S., Minotti, G. and Masotti, L. (1986) Membrane Alterations in Cancer Cells: The Role of Oxy Radicals. *Annals of the New York Academy of Sciences*, **488**, 468-480. https://doi.org/10.1111/j.1749-6632.1986.tb46579.x

[85] Fujiwara, T., Ritchie, K., Murakoshi, H., Jacobson, K. and Kusumi, A. (2002) Phospholipids Undergo Hop Diffusion in Compartmentalized Cell Membrane. *The Journal of Cell Biology*, **157**, 1071-1082. https://doi.org/10.1083/jcb.200202050

[86] Singer, S.J. and Nicolson, G.L. (1972) The Fluid Mosaic Model of the Structure of Cell Membranes: Cell Membranes Are Viewed as Two-Dimensional Solutions of Oriented Globular Proteins and Lipids, Abstract. *Science*, **175**, 720-731. https://doi.org/10.1126/science.175.4023.720

[87] Kusumi, A., Nakada, C., Ritchie, K., Murase, K., Suzuki, K., Murakoshi, H., *et al.* (2005) Paradigm Shift of the Plasma Membrane Concept from the Two-Dimensional Continuum Fluid to the Partitioned Fluid: High-Speed Single-Molecule Tracking of Membrane Molecules. *Annual Review of Biophysics and Biomolecular Structure*, **34**, 351-378. https://doi.org/10.1146/annurev.biophys.34.040204.144637

[88] Gowrishankar, K., Ghosh, S., Saha, S., C., R., Mayor, S. and Rao, M. (2012) Active Remodeling of Cortical Actin Regulates Spatiotemporal Organization of Cell Surface Molecules. *Cell*, **149**, 1353-1367. https://doi.org/10.1016/j.cell.2012.05.008

[89] Sezgin, E. (2017) Super-Resolution Optical Microscopy for Studying Membrane Structure and Dynamics. *Journal of Physics*: *Condensed Matter*, **29**, Article ID: 273001. https://doi.org/10.1088/1361-648x/aa7185

[90] Brisson, L., Gillet, L., Calaghan, S., Besson, P., Le Guennec, J., Roger, S., *et al.* (2011) Na(V)1.5 Enhances Breast Cancer Cell Invasiveness by Increasing NHE1-Dependent H(+) Efflux in Caveolae. *Oncogene*, **30**, 2070-2076. https://doi.org/10.1038/onc.2010.574

[91] Brisson, L., Driffort, V., Benoist, L., Poet, M., Counillon, L., Antelmi, E., *et al.* (2013) NaV1.5 Na^+ Channels Allosterically Regulate the NHE-1 Exchanger and Promote the Activity of Breast Cancer Cell Invadopodia. *Journal of Cell Science*, **126**, 4835-4842. https://doi.org/10.1242/jcs.123901

[92] Morenilla-Palao, C., Pertusa, M., Meseguer, V., Cabedo, H. and Viana, F. (2009) Lipid Raft Segregation Modulates TRPM8 Channel Activity. *Journal of Biological Chemistry*, **284**, 9215-9224. https://doi.org/10.1074/jbc.m807228200

[93] Bobkov, D. and Semenova, S. (2022) Impact of Lipid Rafts on Transient Receptor Potential Channel Activities. *Journal of Cellular Physiology*, **237**, 2034-2044. https://doi.org/10.1002/jcp.30679

[94] Vincze, Gy., Sziget, Gy.P. and Szasz, A. (2016) Reorganization of the Cytoskeleton. *Journal of Advances in Biology*, **9**, 1872-1882. https://cirworld.com/index.php/jab/article/view/4059

[95] Szász, A.M., Lóránt, G., Szász, A. and Szigeti, G. (2023) The Immunogenic Connection of Thermal and Nonthermal Molecular Effects in Modulated Electro-Hyperthermia. *Open Journal of Biophysics*, **13**, 103-142. https://doi.org/10.4236/ojbiphy.2023.134007

[96] Szőke, É., Börzsei, R., Tóth, D.M., Lengl, O., Helyes, Z., Sándor, Z., *et al.* (2010) Effect of Lipid Raft Disruption on TRPV1 Receptor Activation of Trigeminal Sensory Neurons and Transfected Cell Line. *European Journal of Pharmacology*, **628**, 67-74.

https://doi.org/10.1016/j.ejphar.2009.11.052

[97] Danics, L., Schvarcz, C.A., Viana, P., Vancsik, T., Krenács, T., Benyó, Z., *et al.* (2020) Exhaustion of Protective Heat Shock Response Induces Significant Tumor Damage by Apoptosis after Modulated Electro-Hyperthermia Treatment of Triple Negative Breast Cancer Isografts in Mice. *Cancers*, **12**, Article No. 2581. https://doi.org/10.3390/cancers12092581

[98] Glauber, R.J. (1963) Time-Dependent Statistics of the Ising Model. *Journal of Mathematical Physics*, **4**, 294-307. https://doi.org/10.1063/1.1703954

[99] Kawasaki, K. (1966) Diffusion Constants near the Critical Point for Time-Dependent Ising Models. I. *Physical Review*, **145**, 224-230. https://doi.org/10.1103/physrev.145.224

[100] Kim, S., Yu, J., Kang, J., Kim, Y. and Ko, T.Y. (2024) Current Understanding of Modulated Electro-Hyperthermia in Cancer Treatment. *Kosin Medical Journal*, **39**, 160-168. https://doi.org/10.7180/kmj.24.127

[101] Astumian, R.D., Chock, P.B., Tsong, T.Y. and Westerhoff, H.V. (1989) Effects of Oscillations and Energy-Driven Fluctuations on the Dynamics of Enzyme Catalysis and Free-Energy Transduction. *Physical Review A*, **39**, 6416-6435. https://doi.org/10.1103/physreva.39.6416

[102] Lovelady, D.C., Richmond, T.C., Maggi, A.N., Lo, C. and Rabson, D.A. (2007) Distinguishing Cancerous from Noncancerous Cells through Analysis of Electrical Noise. *Physical Review E*, **76**, Article ID: 041908. https://doi.org/10.1103/physreve.76.041908

[103] Szasz, A. (2025) Bioelectromagnetism for Cancer Treatment—Modulated Electro-Hyperthermia. *Current Oncology*, **32**, Article No. 158. https://doi.org/10.3390/curroncol32030158

[104] Szasz A. (2020) Challenges and Solutions of Oncological Hyperthermia. Cambridge Scholars Publishing. https://www.cambridgescholars.com/product/9781036429911

[105] Kaskulova, M.Kh., Kreynipa, Yu.M., Solodkiy, V.A., Shevchenko, L.N., Mashkova, Yu.S. and Belokopytov, L.D. (2021) Modulated Electrohyperthermia (Oncothermia) in Treatment of Malignances of Various Localization (Short Literature Review). *Bulletin of the Russian Scientific Center of Roentgenology of the Ministry of Health of Russia*, **21**, 1-20.

[106] Minnaar, C.A., Szigeti, G.P., Szasz, A.M. and Kotzen, J.A. (2022) Review on the Use of Modulated Electro-Hyperthermia as a Stand-Alone Therapy in a Palliative Setting: Potential for Further Research? *Journal of Cancer Therapy*, **13**, 362-377. https://doi.org/10.4236/jct.2022.136032

[107] Minnaar, C.A., Maposa, I., Kotzen, J.A. and Baeyens, A. (2022) Effects of Modulated Electro-Hyperthermia (mEHT) on Two and Three Year Survival of Locally Advanced Cervical Cancer Patients. *Cancers*, **14**, Article No. 656. https://doi.org/10.3390/cancers14030656